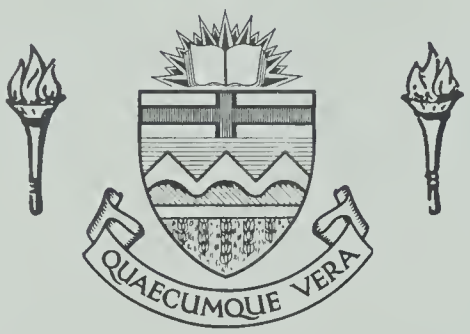

THE UNIVERSITY OF ALBERTA

PHOTOELECTRIC OBSERVATIONS OF THREE W URSAE MAJORIS SYSTEMS

BY

© BARRY BROWN

A THESIS

SUBMITTED TO THE FACULTY OF GRADUATE STUDIES

IN PARTIAL FULFILMENT OF THE REQUIREMENTS FOR THE DEGREE

OF MASTER OF SCIENCE

DEPARTMENT OF PHYSICS

EDMONTON, ALBERTA

SEPTEMBER, 1968

UNIVERSITY OF ALBERTA

FACULTY OF GRADUATE STUDIES

The undersigned certify that they have read and recommend to the Faculty of Graduate Studies for acceptance, a thesis entitled

"Photometric Observations of Three W UrsaeMajoris Systems"

submitted by Barry Michael Brown, in partial fulfilment of the requirements for the degree of Master of Science.

ABSTRACT

Photoelectric observations are described for three W Ursa Majoris systems: VW Cephi, 44i Bootes and W Ursa Majoris, using yellow and blue light. The magnitude variations of the variable stars, determined from the brightness measurements are plotted as light curves from which times of minimum light are determined accurate to about $\pm$ $^{d}.0005$. An examination of the differences between observed times of minimum light and the computed times of minimum light indicates a continued rapid decrease in the period of VW Cephi, a slow increase in the period of 44i Bootes, and further evidence that the period variation of W Ursa Majoris is cyclic.

ACKNOWLEDGEMENTS

I would like to express sincere thanks to my advisor, Dr. E.H. Pinnington for his assistance and guidance in the acquisition of the photometric observations as well as in the preparation of this essay.

Thanks is also due to Dr. G.L. Cumming who's interest in Astronomy, along with Dr. Pinnington's, led to the establishment of facilities for photometric observations.

I would also like to express my gratitude to chief machinist, N. Riebeek and his staff who built the photometer, and other parts essential for satisfactory use of the telescope.

Finally, sincere thanks to L.N. Scotten, who persevered with the cold weather to record the brightness measurements.

TABLE OF CONTENTS

LIST OF ILLUSTRATIONS

LIST OF TABLES

CHAPTER I

INTRODUCTION

The radiation emitted by the stars is the only direct source of information about them. Consequently, the sciences of astronomy and astro-physics have dealt with the analysis and interpretation of information obtained by the various types of measurements of this radiation. Photometry, a branch of astronomy, is concerned with the measurements of stellar brightnesses. Photometry can be usefully employed in many areas of research, such as the establishment of magnitude systems, the acquisition of colour magnitude diagrams for clusters, and the study of variable stars (1). It is the last of these, the study of variable stars, which is the subject of this thesis.

The first photometric work was carried out by the visual method, generally employing some sort of null method (2), for example in the Zollner photometer, the star was compared to an artificial star whose brightness could be made equal to that of the star under study, the brightness of the star could then be read from a calibrated scale. With this method it was possible to obtain the magnitude of a star within a probable error of $\pm\ 0^{m}.04$ (.04 magnitudes). One of the biggest problems with this method was the presence of personal error which resulted in systematic differences between magnitudes measured by various observers.

The development of photographic photometry in the nineteenth century (3) brought about magnitude measurements, which with proper care, were accurate to $\pm 0^{m}.02$.

The basic principle behind photographic photometry is that if light from a star is incident on a plate, the size and blackness of the resulting image should be proportional to the brightness of the star. However, in practise, this type of photometry is seriously limited by the fact that the relationship between stellar brightness and image blackening on the plate is not linear for extreme brightness or faintness of a star. Photographic photometry is still useful today for measurements of the brightnesses of a large number of stars at one time and also for the discovery of variable stars. The most recent form of photometry, the one employed in this project, is photoelectric photometry. Photoelectric photometry was origionally pioneered by Stebbins in 1907 (4). The basic principle behind photoelectric photometry is that light incident on a photoelectric device produces a photo-current which is proportional to the intensity of the incident light. With the recent development of photomultipliers and amplifiers featuring high gain and low noise, photoelectric photometry has become the most accurate form of photometry. Using photoelectric methods it is possible to obtain magnitude measurements accurate to $\pm 0^{m}.01$. The restriction on accuracy of this measurement is brought about mainly by atmospheric

turbulence and changes in atmospheric transparency. Another advantage of photoelectric photometry is that the relationship between light intensity incident on the photocathode of the photomultiplier and the output signal at the anode is linear over a large range of stellar brightness. Consequently, it is possible to obtain more accurate light curves and light elements with photoelectric photometry than with visual or photographic photometry.

The objects of study, by means of photoelectric photometry in the programme described here, are variable stars. The variable stars, which exhibit temporal variations in brightness are divided into two broad classes. These are the intrinsic variables, whose brightness changes due to internal causes, and the extrinsic variables, whose brightness changes due to some factor outside the stellar surface. This thesis describes a programme of measurements of eclipsing variables. An eclipsing variable consists of two or more stars such that each of a pair of stars periodically eclipses the light of the other resulting in the variation in brightness of the system as seen as a whole.
The eclipsing variables are divided into four groups which are named after the prototype stars of each type. These are the U Cephi type, the Algol type, the Beta Lyrae type and the W Ursa Majoris type.

These are characterized by the form of their light curves:

i) U Cephi type - total eclipse at primary minimum, brightness constant or very nearly so in between eclipses.

ii) Algol type - partial eclipse at primary minimum, brightness constant or very nearly so in between eclipses.

iii) Beta Lyrae type - light curve noticeably convex upward between eclipses, period greater than 12 hours, minima may be equal or unequal.

iv) W Ursa Majoris type - light curve noticeably convex upward between eclipses, period less than 12 hours, minima equal or nearly equal.

Typical light curves for variable stars of these types are shown in Fig. 1.1. The division is somewhat arbitrary as it is frequently found an eclipsing variable does not fit uniquely into any of the categories.

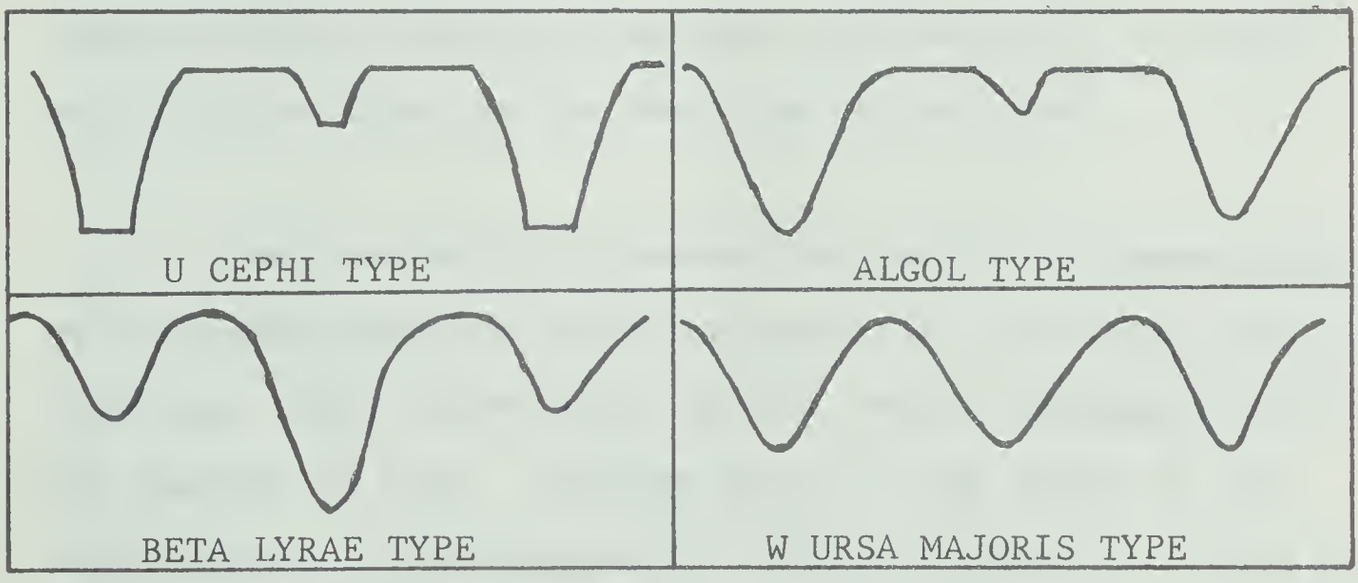

Fig. 1.1 Typical Light Curves of the Four Types of Eclipsing Variables.

In these graphs, the Ordinate is the Magnitude Scale, the Abcissa is the Time Scale.

The prime importance of eclipsing variable stars is due to the fact that observations of these stars provide the most direct source of information about the physical properties of the stars. From the light curve alone one can obtain the relative sizes of the stars, the separation of the components, the surface brightnesses, the degree of ellipticity of the stars and the physical structure of the outer atmospheres of the composite stars. If the distance of the system from the earth is known, then the light curve together with the radial velocity curve can be used to give detailed information about the masses, diameters, temperatures, and other properties of the component stars. The radial velocity curve is obtained by observing the Doppler shift of the lines in the spectrum of the star.

One particularly interesting result of observations of eclipsing variable stars is that it is found for most of them that their light curves do not remain unchanged with the passage of time. Changes occur in the shape of the light curves, or the period of eclipse changes, or there are irregularities in the light curve for a particular cycle. Changes in the shape of the light curve and irregularities

in the light curve are believed to be caused by the following:

i) apsidal motion - rotation of the major axis of an elliptical orbit.

ii) presence of a changing gas shell.

iii) ejection of matter from the star or gas shell.

Changes in the period of the eclipsing binary can be caused by any combination of the following factors:

i) apsidal motion.

ii) perturbation effects due to a third body.

iii) intrinsic variations in the star system such as ejection of matter from the star system.

F.B. Wood (5) has stated that it is still not possible to tell if a given period change is sudden or part of a long range oscillatory change, he also pointed out that lack of measured times of minimum light has not helped to overcome this difficulty. Accordingly it was decided to determine times of minimum light for three W Ursa Majoris systems as a contribution towards the objective of understanding the nature of the period changes more precisely. W Ursa Majoris was chosen since it is the prototype of the W Ursa Majoris type variable and also because the nature of its period variation is still not clear. 44i Bootes and V W Cephi were chosen from a list of 25 variable stars for which times of minimum light were particularly required, prepared by a committee headed by M. Plavec of Ondrejov Observatory, Czechoslovakia (6).

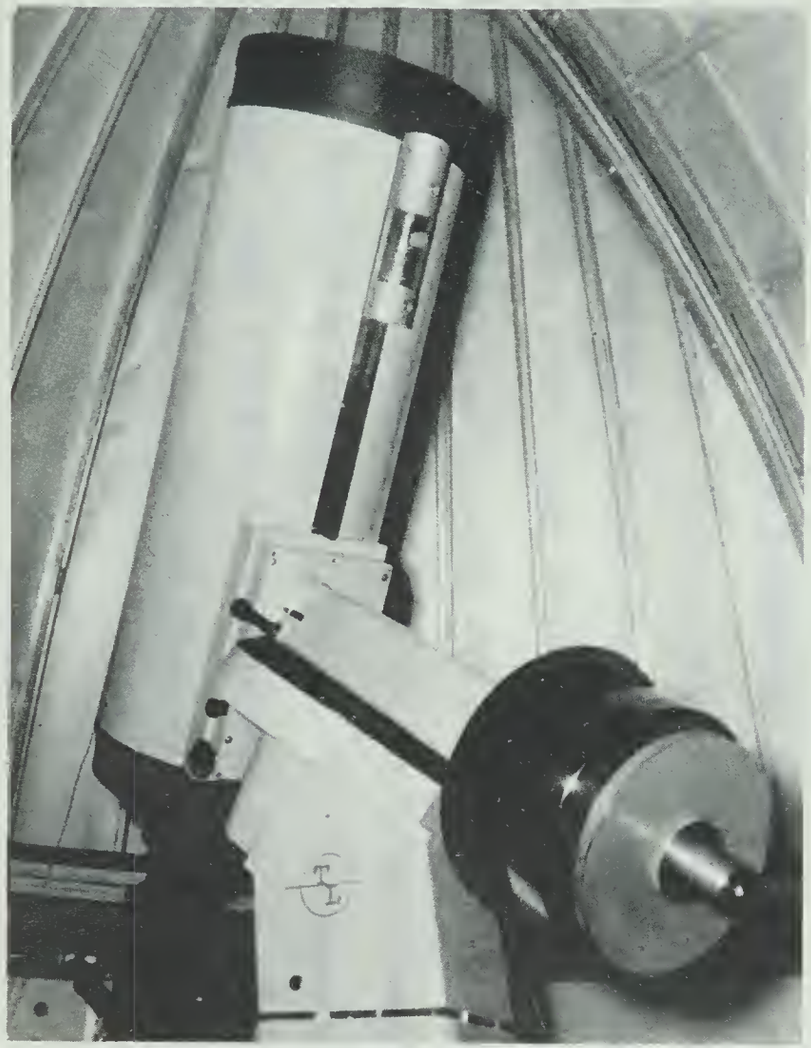

Plate 1.I THE 12½" CASSEGRAIN REFLECTOR

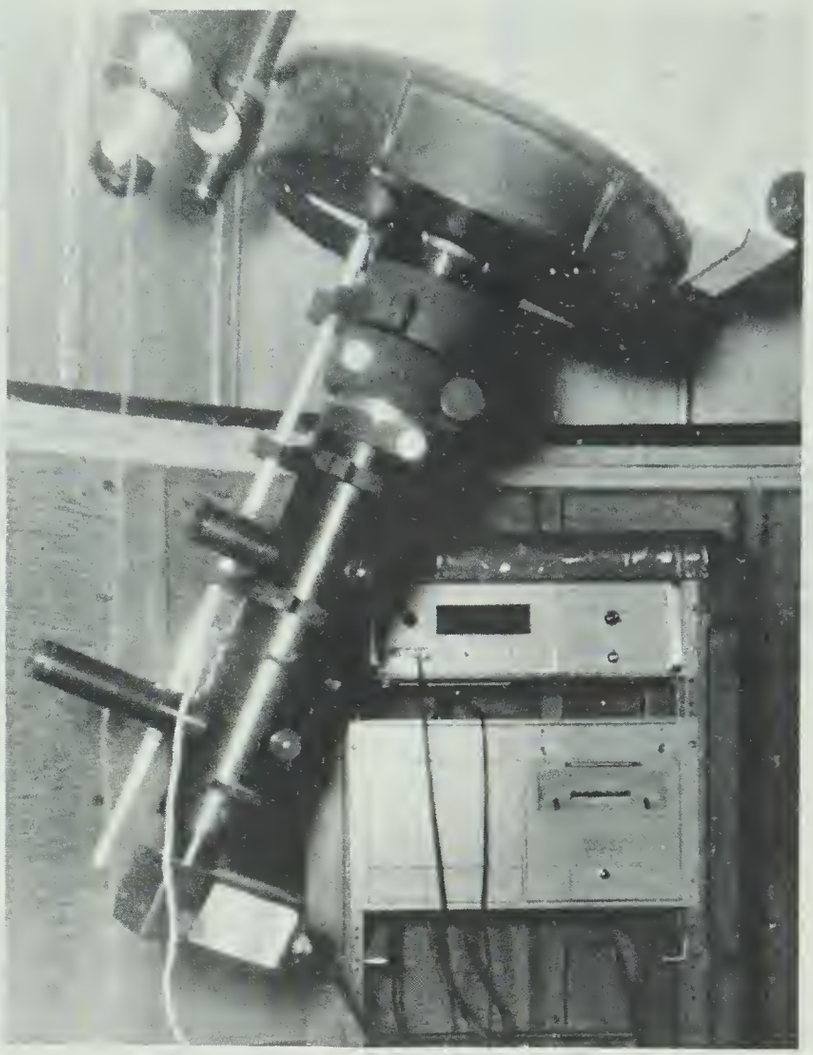

Plate 1.2 THE PHOTOMETER VOLTMETER AND RECORDER

CHAPTER 2

EQUIPMENT AND EXPERIMENTAL PROCEDURE

2. 1 Equipment

The equipment used in the project consisted of the following items:

12½" Cassegrainian telescope

photoelectric photometer

1P21 photomultiplier

digital voltmeter and recorder

high voltage supply

remote print command and coding device

Origionally it had been intended to use a Boonton voltmeter and a Leeds and Northrup Speedomax recorder. The Speedomax recorder was found to be unsuitable in practise. During extremely cold observing weather, the mechanical parts did not move freely and the resulting pen drag error made observations meaningless. It was not practical to use the Boonton voltmeter alone because of the difficulty in reading the meter to an accuracy sufficient for precise magnitude measurements. At best, the accuracy using the Boonton voltmeter was $\pm$ $0^m.05$. In addition the telescope had to be "winterized" as described in the following section. The basic arrangement of the equipment used for the photoelectric observations is shown in the schematic diagram on the next page.

FIGURE 2.1

SCHEMATIC DIAGRAM OF THE EQUIPMENT

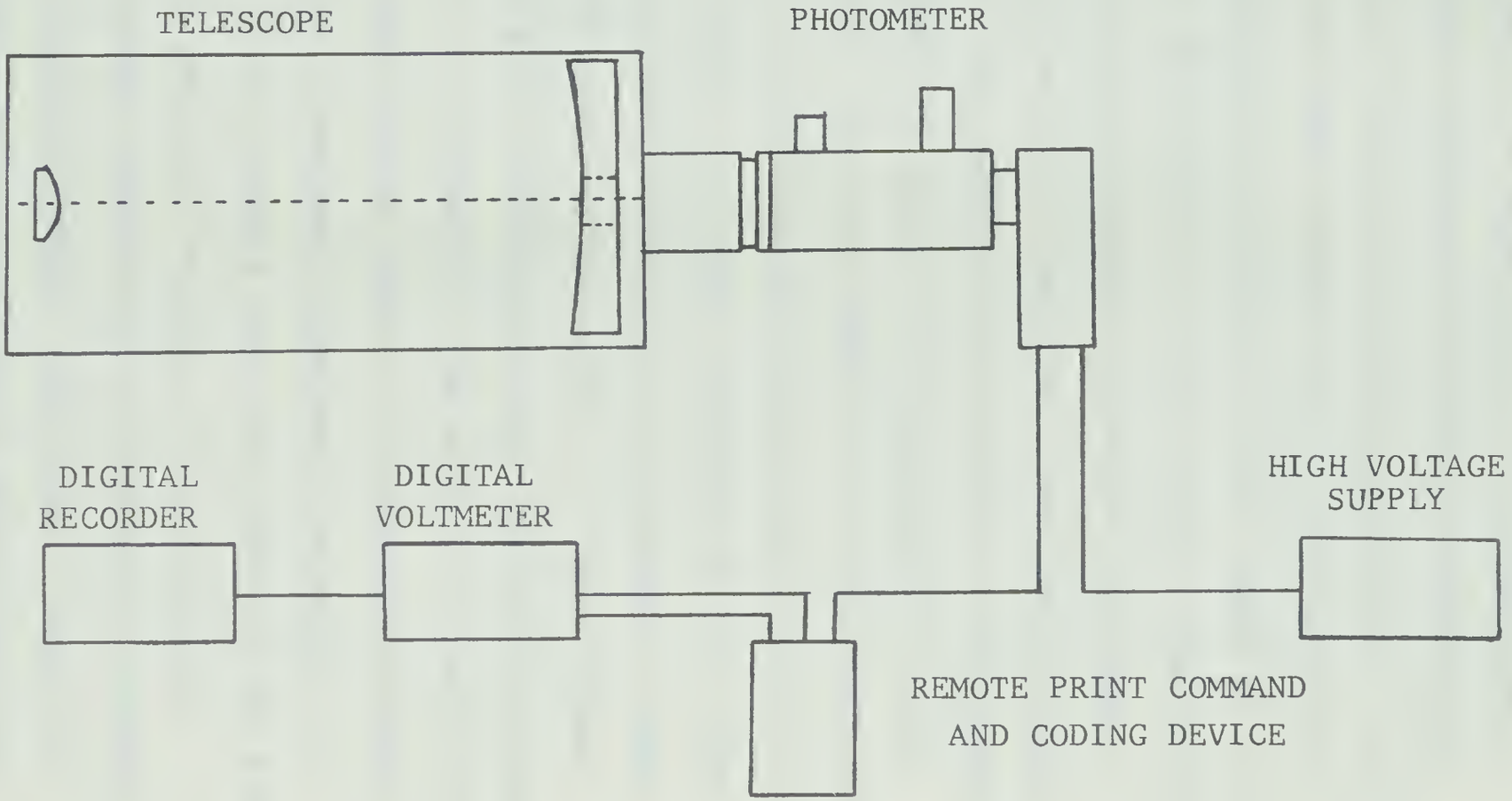

i) The Telescope

The telescope is an equatorically mounted Cassegrainian type reflector obtained from Tinsley Laboratories, Berkeley, California. The optical system consists of a 12½" diameter mirror of 48" focal length and a 3 3/4" secondary mirror which combined give an effective focal length of 192". The right ascension (R.A.) drive is motor driven, the driving rate being controlled by a frequency converter which can deliver a.c. voltages within a frequency range centred about 60 cycles / second. Two controls are provided on the telescope to facilitate bringing the object of study into the centre of the field of view. The first control is a fine adjustment to the declination by which the declination may be varied by $\pm$ 5°. The second control is a fine adjustment to the right ascension drive rate, thus permitting the telescope to gain or fall behind the rotation of the earth. A 1 3/4" finder telescope is provided for locating the star field of interest. A 3" guide - scope is provided for the purpose of positioning the object to be viewed in the centre of the main telescope's field of view and for subsequent adjustments necessary to correct departures of the objects from the centre of the field. Such adjustments are necessary because of the inevitable irregularities in the R.A. drive rate or inaccurate alignment of the polar axis of the telescope. The guide - scope is equipped with an illuminated cross hair to facilitate this

work.

In the initial period of telescope operation, the teeth on the motor worm gear became stripped and the R.A. drive consequently ceased to function. It was found that the torque applied to the motor worm gear became excessive in cold weather, due to increased viscosity of the grease used between the polar worm gear and the polar worm and possibly to misalignment of these gears due to shrinkage of the metal. Furthermore, when the R.A. of the telescope was changed manually, there was considerable frictional torque due to the increased viscosity of the grease between the polar worm gear and the polar axle. In order to overcome these difficulties it was decided to install a heating element inside the equatorial housing in the proximity of the polar worm, worm gear, and axle. In this manner the grease between these parts could be kept at a sufficiently high temperature so that friction remained reasonably low. There was never any heating of the observatory due to the heating element or any excessive heating of the equatorial housing in the proximity of the heating element.

ii) The Photometer

A schematic diagram on page 12 shows the components of the photometer which are discussed below. The photometer was designed and built at this university employing basic

FIGURE 2.2
SCHEMATIC OF THE PHOTOMETER

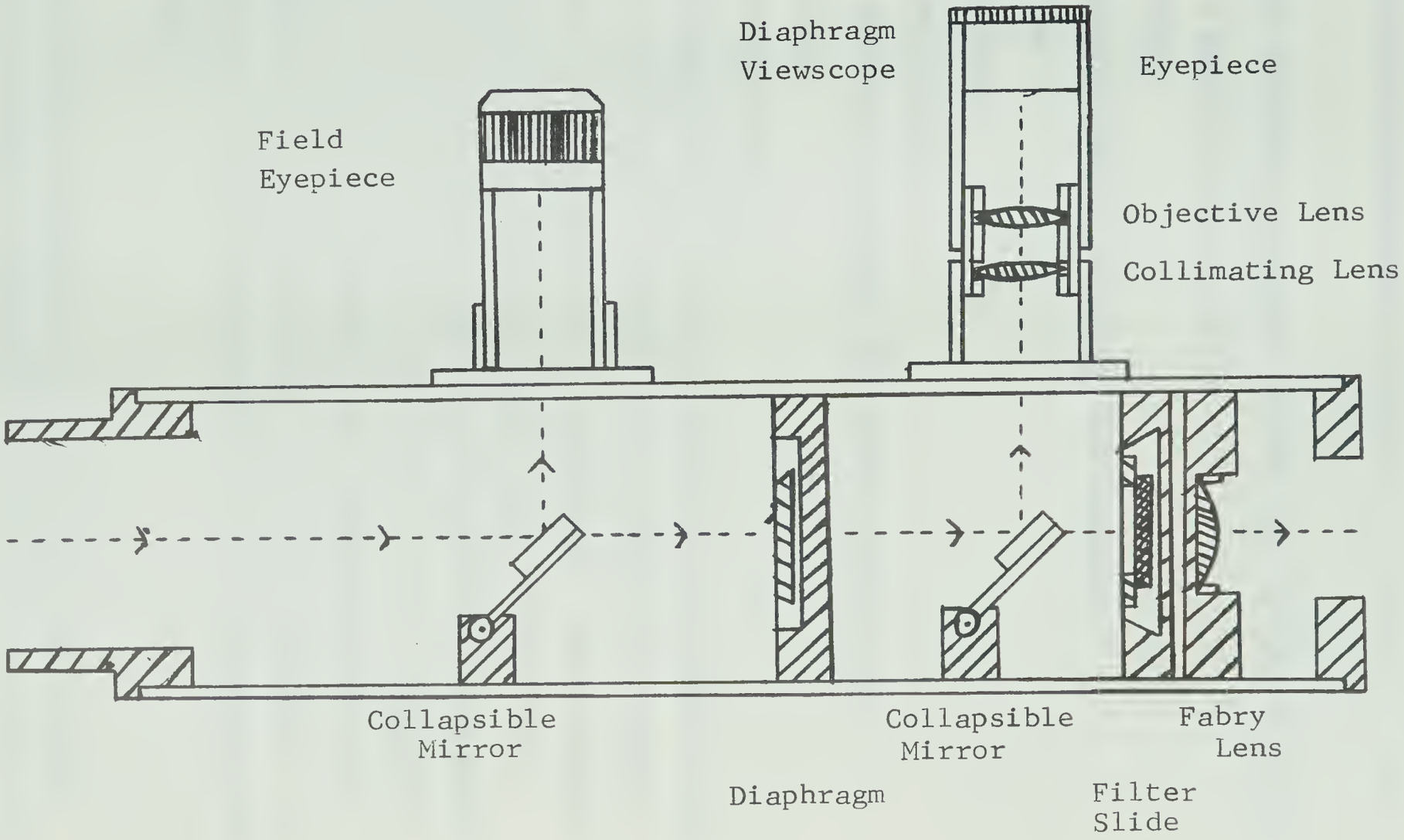

features described in photometer design by Johnson (7) and Code (8).

The photometer basically consists of the following components:

field eyepiece and assembly

diaphragm

diaphragm viewing telescope and assembly

filters

Fabry lens

photomultiplier

The details of these components and their purpose are explained below.

Field Eyepiece and Assembly

A collapsible mirror can be placed in the path of the light beam to view the star field. This permits the object of observation to be centred in the diaphragm. The focusing tube can be adjusted to obtain a sharp image of the field. In practise for the variable stars investigated in this programme, it was found to be more convenient to use the guide - scope for the purpose of centering the observation star in the diaphragm, as the observed stars were fairly bright. For fainter stars use of the field eyepiece for this purpose would be more suitable.

Diaphragm

Usually it is desired to view the light of a single object, for this reason a diaphragm is necessary to block off

all of the field except that containing the object of interest. The diaphragm is located at the focal plane of the telescope. Three holes of diameter 1 m.m., ½ m.m. and ¼ m.m. were drilled into a metal strip so that fields of view of 40", 20" and 10" of arc respectively could be isolated. In the present work the 40" of arc hole was used in order to make sure all the light of a particular star passed through. This was necessary because of the slight shimmy in the telescope mounting which resulted in variation of the position of the star in the diaphragm. If the steps, which are being taken to rectify this fault of the telescope mounting, are successfull, it should be possible to use the 20" of arc diaphragm regularly. On nights of extremely good seeing the 10" of arc diaphragm could be used resulting in more accurate brightness measurements.

The Diaphragm Viewing Telescope and Assembly

A collapsible mirror is provided so that the diaphragm aperture and light beam from the telescope can be reflected upward to the viewing telescope. A collimating lens of 120 m.m. f.l. is positioned at a distance from the diaphragm equal to its focal length, thus producing a parallel beam. A telescope, consisting of an achromatic field lens of 100 m.m. f.l. and an eyepiece, is placed behind this lens. All lenses are contained in the one cell. Of course it is necessary to be able to see the diaphragm if the star under observation is

to be centred in it. For this purpose, a light is positioned to illuminate the diaphragm. A switch is used to alternately turn on the reticle light in the guide - scope and that in the photometer. This lessens the possibility of damage to the photomultiplier which would result if the diaphragm illuminating light was directly incident on the photocathode. With the collapsible mirror in the observing position and the blue filter centred in the photometer, the light seen by the photomultiplier due to the diaphragm illuminating light is equivalent to that of a 6th magnitude star.

The Filter Assembly

Three 1" square filters (ultraviolet, blue, and yellow) are mounted in a slide, so that observations through each filter can take place in sequence. The filters used are those prescribed for measurements in the UBV magnitude system, these are 2 m.m. UG-2 for ultraviolet (U), 2 m.m. GG13 + 1 m.m. BG12 for blue (B), 2 m.m. GG14 for yellow or visual (V). These filters can be obtained from Jena Glassworks, Mainz, Germany. The magnitudes observed with these filters can be linearly transformed to those of the standard UBV system as outlined by Hardie (9). The filters are correctly centred by a ball and socket arrangement in which a sprung ball bearing fits into a socket on the filter slide whenever a filter is centred in the path of the light.

The Fabry Lens

The Fabry lens is required to project an image of the illuminated telescope mirror on the photocathode of the photomultiplier. If the stellar image is focused directly on the photocathode, wandering of the star image in the diaphragm would result in motion of the image over the photocathode with subsequent variations in the output signal due to variations in sensitivity across the photocathode surface. The image size is required to be greater than 1/8" so that the light will not be incident entirely on a region of low sensitivity of the photocathode surface, and must not be greater than 1/4" so that all of the light from the star falls on the photocathode. For this purpose a plano - convex quartz lens of 100 m.m. f.l. is used to produce an image whose size is within these limits.

The Photomultiplier

In the 1940's the 1P21 photomultiplier developed by RCA came into use in photometry due to its advantages of high internal gain ($A = 10^5 - 10^6$) and relatively low noise levels. It has been in use ever since . As has been mentioned previously, it is used with the filters mentioned above for magnitude measurements in the UBV system. Initially measurements were made with an RCA 1P21, however, when the gain of this tube became unstable, a Sylvania 1P21 was employed. The sensitivity of the Sylvania 1P21 was 1/3 that of the RCA 1P21.

FIGURE 2.3 PHOTOMULTIPLIER & HOUSING
AND THE PHOTOMULTIPLIER CIRCUIT

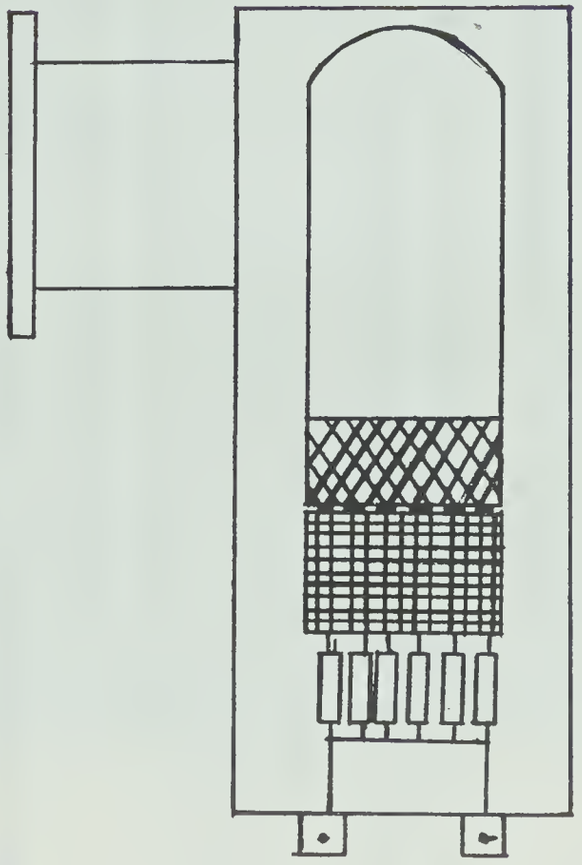

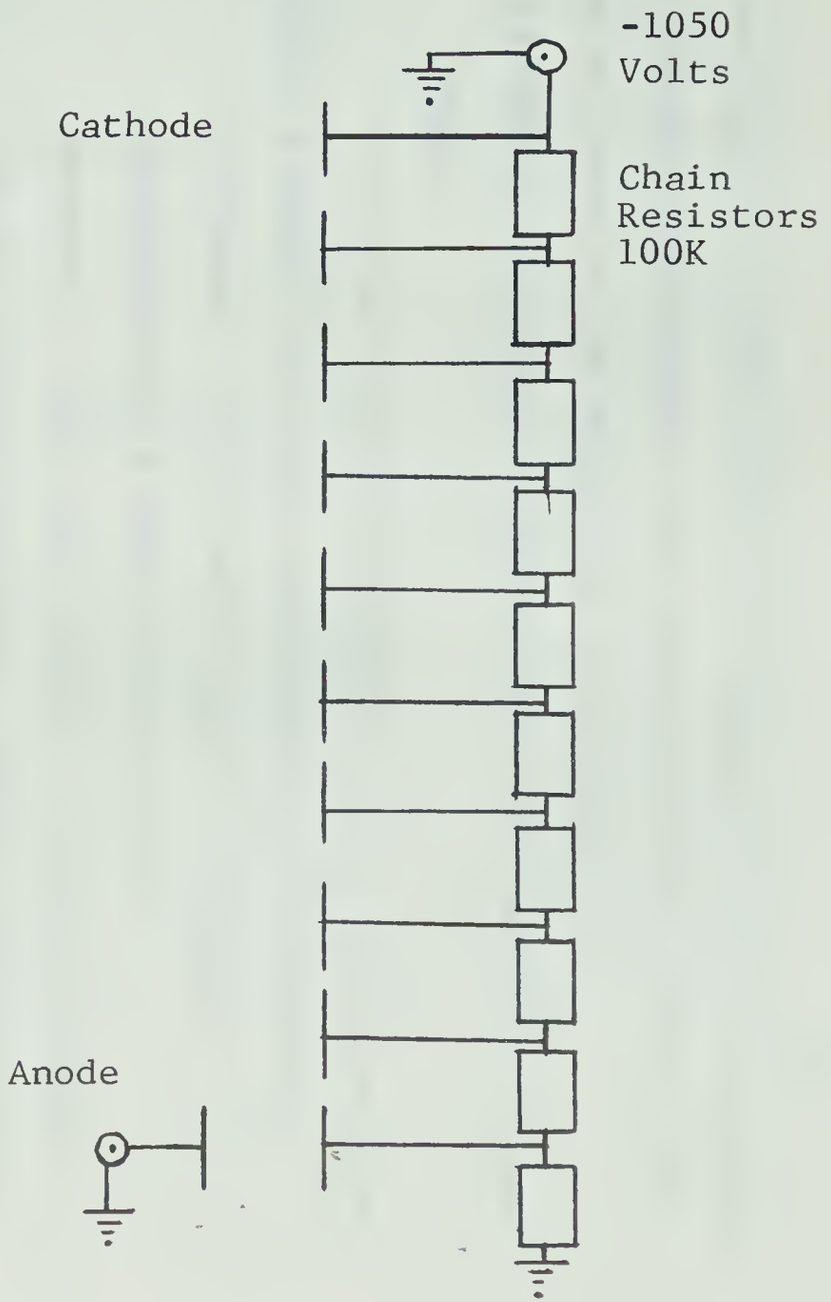

A voltage of - 1050 volts d.c. was employed for the purpose of biasing the dynodes. The characteristics of the 1P21 can be found in the RCA photo tube manual.

iii) Digital Voltmeter, Digital Recorder and High Voltage Supply

All three pieces of equipment were obtainted from Hewlitt Packard, and their description is as follows:

Voltmeter - type 3440A digital voltmeter equipped with a 3441A plug in unit.

Recorder - type 562A digital recorder equipped for six column operation. Signals are recorded in four columns.

High Voltage Supply - Harrison 6515A d.c. power supply with voltage range $\pm$ 0- 1700V D.C.

The specifications for these instruments can be found in the 1968 Hewlitt Packard catalogue.

With the 3441A plug in unit the output signal could be recorded to $\pm$ 1 mv. Since the completion of observations the 3441A plug in unit has been replaced by a 3443A plug in unit so that output signals can now be read to $\pm$ .01 mv. This should provide more precise measurements of the fainter stars.

iv) The Remote Print Command and Coding Device

The device essentially consists of one switch connecting either the photomultiplier output to the digital voltmeter or the 7.5 volt d.c. supply to the recorder, and another

Plate 2.1 Remote Print Command and Coding Device

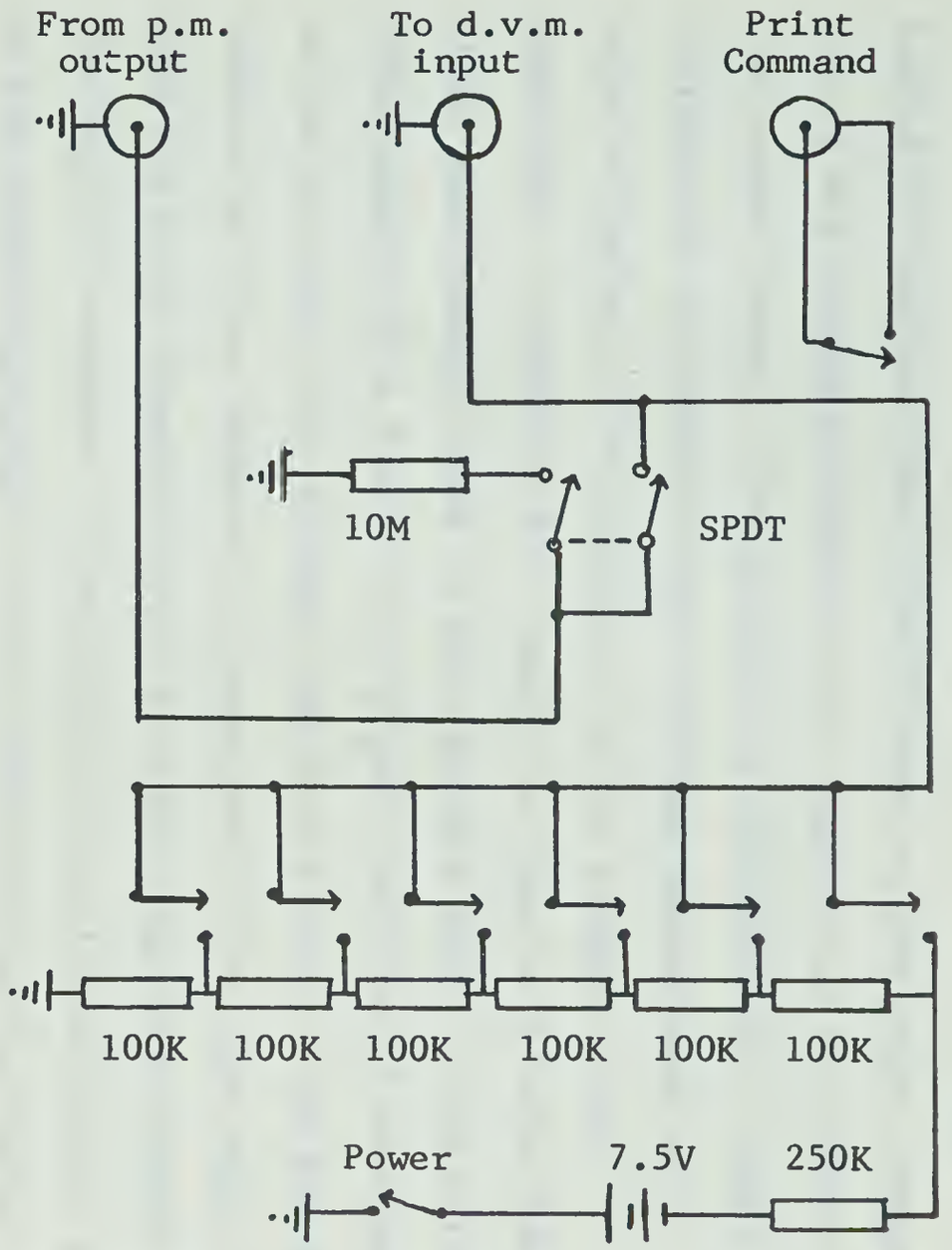

Figure 2.4 Circuit Diagram of Coder

switch to complete the circuit known as the print command. Any of six voltages from the d.c. supply can be printed on the output record. The purpose of recording d.c. supply voltages is to identify each recorded measurement on a star or the sky. For example, in the program to be described, a recorded d.c. supply voltage of 6 volts identified measurements made on the variable star. This followed subsequently by a 3 volt d.c. signal indicated a measurement on the variable star through the blue filter. The switch labeled as print command is connected to the line which transmits the print command pulses from the digital voltmeter to the digital recorder. (For further details see figure 6-10 of the operating manual for the 3440A digital voltmeter.) Using this device it is possible to place the recording equipment in a convenient position in the observatory. Another purpose of this device is to correlate the recorded measurements with the times of observation of the variable star, which were recorded by hand at the observing end of the telescope. It is hoped a digital clock can be installed in the digital recorder, which would permit the time of observation to be recorded simultaneously with the brightness measurements.

2.2 Systematics and Procedures

i) The Magnitude System

About 120 B.C. the Greek Hipparchus set up a magnitude system consisting of six groups such that the first magnitude was assigned to the brightest stars and the sixth magnitude was assigned to the faintest stars. The magnitude system has been in use in classifying stellar brightnesses ever since. In the nineteenth century Pogson noted that a first magnitude star gives about 100 times as much light as does a sixth magnitude star. Since the response of the eye is logarithmic, he suggested that a change of one magnitude corresponded to an intensity ratio of $(100)^{.2}$ or 2.512. Hence the relationship between magnitude differences and intensity ratios should be given by the following expression.

$$m_1 - m_2 = -2.5 \log_{10} (I_1/I_2)$$

The above mathematical relationship between magnitude difference and intensity ratios is used at present. Hence, in principle, once the brightnesses of two stars are measured by photometric methods, the magnitude difference between these stars is readily determined. The observed magnitude of a star will depend on the colour sensitivity of the photometric equipment employed, in particular, the measured magnitude of a star will depend on the reflection or transmission properties of the telescope's optics, the colour sensitivity of the photoelectric device, the transmission

properties of the filters used for observation, and the sensitivity of the amplifiers. Consequently, it can be seen every telescope defines its own unique magnitude system. If the colour sensitivity of a particular instrument closely approximates that of the instrument(s) used to define a particular magnitude system it is a comparitively simple task to convert the observed magnitudes to magnitudes in the standard system by means of linear transformations. The UBV magnitude system established by Johnson and Morgan (10) is the magnitude system usually used for work on the variable stars. Hence, the photometer used in the present project was equipped for observations in the UBV magnitude system. It was not necessary to transform the observed magnitudes into the standard UBV system in this project since only times of minimum light were being sought.

ii) The Use of Comparison Stars and Calibration Stars in Photometry

The current output of the photoelectric device used in photometry is proportional to the observed brightness of a star, so that the relationship between magnitude and output signal is $m = S - 2.5 \log_{10} E$

E = signal reading S = amplifier sensitivity

S will depend on instrumental parameters (colour sensitivity of the filters, photoelectric device, and the elements of the amplifier) and thus may not remain constant during a night's

observations, it is also likely that S will change from day to day. For this reason, the magnitude of a star is not readily fitted into the UBV system by absolute photometry, which in itself is a time consuming and very demanding task. Instead, the practise in variable star work is to select a comparison star located as close as possible to the variable. The ratio of intensities, which are obtained, can then be used to determine the magnitude difference between the variable and comparison stars. Provided the brightness of the comparison star is constant, a plot of the magnitude difference between the comparison and variable stars vs time shows the variation in magnitude of the variable star. In order to verify that the light of a comparison star is constant, the brightness of a calibration star is measured on two or more occasions during a given night. The observed magnitude differences between these stars should agree within the limits imposed by the atmosphere $\pm\ 0^{m}_{.}01$. The optimum choice of a comparison star is one which is as close as possible to the variable star and has about the same brightness and colour (spectral class) as the variable. The colour sequence blue - white - yellow - red corresponds to the spectral class sequence O B A F G K M. By choosing a star with these properties, errors due to extinction by the earth's atmosphere and systematic errors due to the possible non-linearity of the photoelectric equipment are minimized.

Data on the comparison and variable stars are listed below and the relative position of the variable stars and comparison stars are shown in the star charts.

Plate 2.2a Field of VW Cephi

Table 2.2a Variable and Comparison Star Data for VW Cephi

Star	R.A.(1900)	Dec.(1900)	Mag.	Spec.Class
VW Cephi	$20^h38.6^m$	+75°13'	8.1	G5
BD75°753	$20^h40.6^m$	+75°32'	8.07	KO

Plate 2.2b Field of 44i Bootes

Table 2.2b Variable and Comparison Star Data for 44i Bootes

Star	R.A.(1950)	Dec.(1950)	Mag.	Spec.Class
44i Bootes	15^h05^m	+48°03'	4.86	G2
39 Bootes	$14^h47^m59.2^s$	+48°55'31"	6.10	F6

Plate 2.2c Field of W Ursa Majoris

Table 2.2c Variable and Comparison Star Data for W Ursa Majoris

Star	R.A.(1900)	Dec.(1900)	Mag.	Spec.Class
W.U. Ma.	$9^h36^m44^s$	56°24.5'	8.3	F8
BD56°1399	$9^h35^m40^s$	56°06'	8.7	KO

The comparison star used for VW Cephi BD75°753 has been observed to have variable light. Dugan (11), Swope (12), and Kordylewski (13) have found magnitude variations between $0^m.4$ and $0^m.6$, on the other hand Walter (14) has found no variations. On the two nights when a calibration star BD75°750 was also measured no variations in the comparison star could be detected within the limitations of the measurements.

39 Bootes was used as the comparison star for 44i Bootes. In the past HR5581 has been used by various observers as the comparison star. On the two nights when HR5581 was used as the calibration star, no variations in the comparison star could be detected within the limitations of the measurements.

The comparison star for W Ursa Majoris, BD56°1399 was found to be of constant brightness by Schmidt and Schrick (15). In the present work, no variation in brightness was detected within the limitations of the measurements.

iii) Extinction Corrections

In passing through the earth's atmosphere, part of the stellar light is scattered and absorbed. The resulting attenuation of the light is a function of the extinction coefficient and the air mass through which the light travels. The extinction coefficient depends on the wavelength region observed. The air mass is a function of the zenith angle of the observed star.

The relationship between the true apparent magnitude of a star (its apparent magnitude outside the earth's atmosphere) and observed apparent magnitude is to a first approximation,

$$m_t = m_o - KX = S - 2.5 \log(E) - KX$$

m_t = true apparent magnitude m_o = observed apparent magnitude

S = amplifier sensitivity K = extinction coefficient

X = relative air mass = secz = $(\sin(\phi) \sin(d) + \cos(\phi) \cos(d) \cos h)^{-1}$ $(z < 65°)$

z = zenith angle, h = hour angle of star, ϕ = latitude of observer, d = declination of the star.

Hence, the relationship between observed magnitude difference and true magnitude difference between the variable and comparison star is given by

$$m_{t_v} - m_{t_c} = m_{o_v} - m_{o_c} + K \Delta X$$
$$= - 2.5 \log(E_v/E_c) + K \Delta X$$

A detailed discussion of the extinction corrections and extinction coefficients is given by Hardie (9).

In the cases of VW Cephi and W Ursa Majoris, the relative air mass difference, Δx, between the variable and comparison stars was assumed to be negligible, so that extinction corrections were deemed to be unecessary. This is justified by the small angular seperations of the variable and comparison stars. The seperation between 44i Bootes and 39 Bootes was considerably larger so that extinction corrections were deemed necessary in this case. 39 Bootes was not

observed through a sufficient range of air masses to determine the blue and yellow extinction coefficients experimentally. Therefore, it was decided to adopt values of .25 for the yellow extinction coefficient K_V and .35 for the blue extinction coefficient K_B. These are mean values for an altitude of 2200' (16) , the altitude of Edmonton is 2185'. The extinction coefficients vary during the course of a night at most sites so that experimentally determined coefficients at best represent mean values for the night. Consequently, the assumed extinction coefficients give corrections of the same merit as experimentally determined coefficients. The resulting corrections were then added to the observed magnitude differences. The corrections were all found to be less than $0^m.01$, and were thus within the limits of experimental accuracy.

iv) Heliocentric Times

As the Earth proceeds in its orbit around the Sun the distance between the Earth and a given variable star changes. Consequently, for given light elements one finds a cyclic deviation of observed times of minimum light from those computed using the light elements. This is not critical for observations of long period variable stars whose periods can only be resolved to within a few days, however, the effect is readily detectible in short period variable stars. In order to eliminate this effect it is necessary to calculate

the times of minimum light which would be observed from the Sun. In order to do this a time increment is added to the geocentric time of an observation to obtain the heliocentric time of observation. The mathematical relationship (17) which has been derived for this time increment is

Δt = heliocentric time - geocentric time

= - 8.31 R cos Θ cos B cos l - 8.31 R sin Θ cos B sin l

R = distance from the Earth to the Sun (in astronomical units)

Θ = position of earth on ecliptic referred to the vernal equinox

l = longtitude of the star on the ecliptic

B = latitude of the star referred to the ecliptic

B and l can be transformed into coordinates on the celestial sphere as follows

cos B cos l = cos d cos a

cos B sin l = sin e sin d + cos e cos d sin a

d = declination of the star

a = right ascension of the star

e = inclination of the ecliptic = 23°27'

Values for R and Θ can be found in the American Ephemeris and Nautical Almanac.

v) The Time Scale for Observations

In order that the observations of various observers can be compared directly, the times of observation are recorded in heliocentric Julian days. The Julian date is equal to the number of days which have elapsed since noon on January 1

4713 B.C. at Greenwich. To determine the heliocentric Julian date of an observation the following procedure is followed:

i) the local time is converted to G.M.A.T. (for Edmonton this means adding 7 hours to the local time.)

ii) the heliocentric correction is then added to this time to obtain the heliocentric time

iii) the resulting times are expressed in Julian days (the beginning of a Julian day is at 12 noon at Greenwich). The Julian date for each day of the year can be found in the American Ephemeris and Nautical Almanac.

vi) General Observing Techniques

On nights of good seeing when there was no change in sky brightness the procedure was as follows: observations were made of the sky in blue, then in yellow, then observations were made of the comparison star in blue and yellow, finally observations were made on the variable star in blue and yellow. On nights when seeing was not very good or the sky brightness was changing, each set of measurements on the variable and comparison stars was preceded and followed by measurements of sky brightness. A complete set of such measurements could be completed in 4 - 6 minutes. At the time when only the digital voltmeter was available the recorded measurements of a star's brightness were those judged by the observing assistant to represent the mean signal, and the recorded time of observation was the time at which the judgement was made. Once

the digital recorder was available the procedure was to record a sample of the output signal for a certain time interval, 5 seconds for each sky reading, 10 seconds for each reading on the comparison and variable stars. In this case the time recorded as the time of observation of the variable was the time at the mid point of the observation of the variable. No assistant was required for this portion of the project. In order to determine the hour angles of the stars (the hour angle is used in computing the air mass, which in turn is used to determine extinction corrections), the sidereal time was recorded from the sidereal clock once during the night. On those nights when a calibration star was observed, measurements were made on the calibration star twice during the night.

vii) Reduction of Data

For each set of observations in a particular colour, the mean sky brightness reading, obtained from measurements before and after a measurement of the comparison or variable star, was subtracted from the star plus sky brightness reading to obtain the star brightness reading of the comparison or variable star. Then the mean brightness reading for the comparison star, as determined from measurements before and after the measurement of the variable star, was used with the brightness reading for the variable star to determine the magnitude difference between the comparison and variable star

as outlined in the discussion of the magnitude system. As has been mentioned previously, extinction corrections were applied only in the case of 44i Bootes. The time of each observation of the variable star was converted into heliocentric times by means of the formula stated in the discussion of heliocentric time. The results were then displayed in the form of light curves of magnitude difference vs time (in heliocentric days) for both colours. The times of minimum light were then found by forming chords joining points on the light curve of equal magnitude before and after the mid point of eclipse. The mid point of each chord gave a value for time of minimum light. A mean of these times was taken to be the time of minimum light. For short period variables it is expected the time of minimum light should be the same in all colours, hence, the use of two colours acted as a check on the accuracy of the determined times of minimum light.

viii) The Graph of Observed minus Computed Times of Minimum Light

If the initial epoch for time of minimum light (expressed in Julian days) is T_o and the period is judged to be P_o (expressed in days) then future times of minimum light can be predicted from the following light element

$$T_n = T_o + nP_o \qquad n = \text{an integer}$$

However, as has been mentioned before, the periods of most

variable stars vary in the course of time so that observed and computed times of minimum light will not necessarily agree. A plot of the observed minus computed times of minimum light vs time (in Julian days) constitutes what is known as an O-C graph.

ix) Analysis of an O-C Graph to determine the Nature of Period Changes

The O-C graph consists of a set of discrete points. However, if the points are fairly accurately determined, a smooth curve can be drawn through these points. The curve can then be analysed to obtain an estimate of the difference between the actual and computed period, and also the time rate of change of the period.

As has been stated above, the computed times of minimum light are given by $T_n = T_o + nP_o$.
More generally the time t at which the phase angle of the system is computed to be ϕ can be expressed in Julian days as

$T = T_o + (t/P_o)P_o$. The observed time at which the phase angle is ϕ is

$$T' = T_o + \frac{1}{\overline{P}} \int_o^t P(t)dt \simeq T_o + \frac{1}{\overline{P}_o} \int_o^t P(t)dt$$

Where $\overline{P}$ is the average value of the period in the interval 0 to t, and P(t) is the period as a function of time.

The difference between observed and computed times at which the phase angle is ϕ is

$$\Delta T' = T' - T = \frac{1}{P_o} \int_o^t P(t)dt - t$$

The time derivative of ($\Delta T'$) is thus

$$\frac{d}{dt} (\Delta T') = \frac{P(t)}{P_o} - 1 = \frac{P - P_o}{P_o} = \frac{\Delta P}{P_o}$$

Hence, the slope of the O-C graph, at a particular time t is proportional to the difference between actual and computed periods at time t.

Taking the second derivative with respect to time we have

$$\frac{d^2}{dt^2} (\Delta T') = \frac{1}{P_o} \frac{d}{dt} (\Delta P) = \frac{1}{P_o} \frac{dP}{dt}$$

Hence, the second derivative of the O-C graph is proportional to the time variation of the period.

In practise the O-C graph consists of scattered points so that the accuracy of the curve drawn through these points is limited. Consequently, only a quantitative analysis of time variations of period can be made.

The example below will indicate these points.

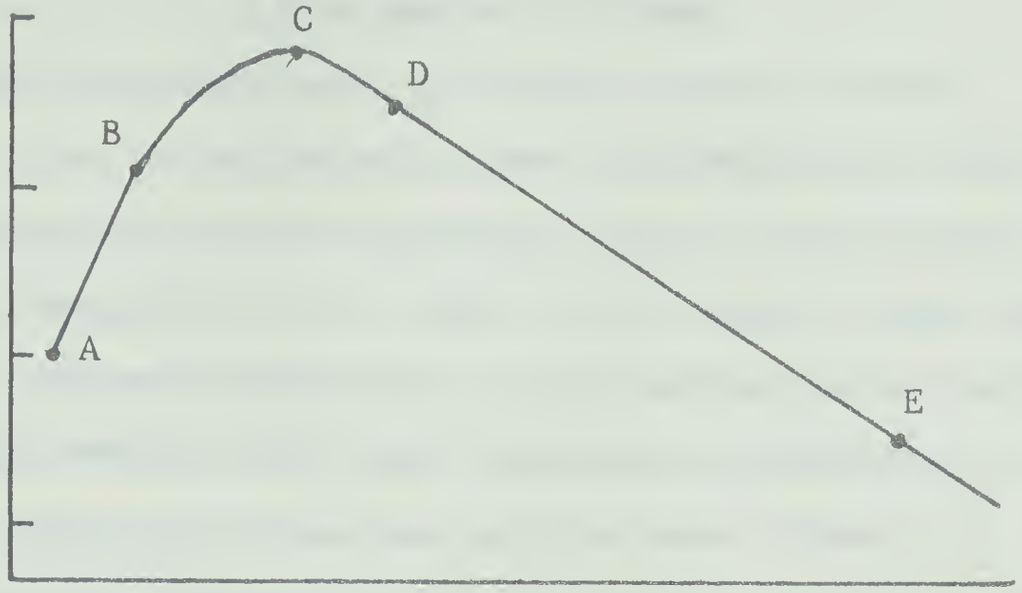

Figure 2.5 Typical Graph of Observed minus Computed Times of Minimum Light

It is assumed the initial epoch is at point A. At point A the slope is positive indicating that the actual period is greater than the assumed period. Between A and B the slope remains constant indicating no period change. Between B and D the slope changes from a positive value to a negative value indicating the period changes from values greater than the assumed period to a value less than the assumed period. In particular at C the slope is 0 indicating the period at that time is equal to the assumed period. The time derivative of the slope assumes large negative values between the points B and D indicating a rapid change in the period. From point D to E, the period again maintains a constant value (no change in slope with time) but the actual period is less than the assumed value (negative slope).

CHAPTER 3

W URSA MAJORIS SYSTEMS

i) The Characteristics of W Ursa Majoris Systems

As is indicated by their extremely short periods, the seperation of the component stars is very small, in most cases comparible to the radii of the stars. Most component stars of these systems have been observed to be dwarf stars of high density with radii and masses comparible to the sun. Their spectral classes are of the later types F, G, K. Due to the close proximity of the stars, the gravitational forces distort the stars into oblate shapes and in many cases the systems are near the limit of dynamic stability. On account of this last factor, there is often ejection of matter from the system or transfer of matter from one of the component stars to the other. This may result in intrinsic changes in the period of a star system of this type.

ii) The Light Curve of a W Ursa Majoris Star

In the simplest theoretical case of an eclipsing binary, where two spherical stars revolve about their centre of mass in circular orbits with no reflection effects, the shape of the light curve depends only on the ratio of the radii of the stars, the ratio of the surface brightnesses and the fractional areas covered in an eclipse. In between eclipses the light of the system should remain constant. However, in the case of W Ursa Majoris systems, the close proximity of the stars gives rise to various effects which

complicate the light curve. The close proximity of the components results in distortion of the stars into ellipsoids, as a result the observed areas and consequently the observed brightnesses are continually changing with time. Furthermore, the gravitational distortion also alters the radiation distribution of the stellar surfaces. A significant amount of light of each of the stars is reflected by the other and since the observed reflecting areas are changing with time, the brightness also changes for this reason. Among other factors affecting the shape of the light curve are darkening at the limb, the tidal effect, and possibly intrinsic variation of the component stars. Frequently, it is also found that there are irregularities in the shape of the light curve. At present, it is thought that these irregularities might be due to the ejection of gas from one of the component stars. Displacements of the secondary minimum from the expected time of minimum light have been observed but as yet are still not explained. The methods of analysis of the light curve of an eclipsing variable to find the quantities characterizing the system are outlined by Binnendijk (18), a more detailed analysis has been given by Kopal (19).

iii) Problems of W Ursa Majoris Systems

The problems raised by the W Ursa Majoris stars for astrophysics are the following:

i) to explain the irregularities in the light curves

ii) to explain the period variations

iii) to predict the evolution of such systems

Kuiper (20) in his theory of contact binaries maintains that periods may vary for any of the following reasons:

i) mass transfer from one component to the other

ii) loss of mass and momentum due to the ejection of matter from the system

iii) pressure at the interface between the two components

The first two factors are satisfactory in explaining the shortening of the period, the third factor is satisfactory in explaining period changes due to rotation of the apsides. However, Kuipers theory suggests no mechanism which would account for increases in period.

F.B. Wood (5) has pointed out that causes of period change can be classified as follows:

i) period changes due to apsidal motion

ii) periodic change of period caused by motion of the system about a third body

iii) erratic and sudden changes in period caused by instability of the system

He suggests that gases ejected from a component star origionate from parts of the stellar surface which are outside the Jacobi limiting surface (21) (within the Jacobi limiting surface, stellar configurations are stable). He

then points out that both increases and decreases in period might be explained by the ejection of gases, which could increase or decrease the momentum of a star depending on whether the gas was ejected in the direction of orbital motion or in the direction opposite to orbital motion. It is not easy to determine the cause of period variations for a given variable star. This was pointed out by F.B. Wood (5) who noted that it cannot always be decided if a given change in period is sudden or part of a long range oscillatory change, and by Eggen (22) who noted that up to 1948 it was still not possible to segregate changes of period resulting from a long range period orbital motion and those due to intrinsic changes. Both these authors have pointed out the need for more photometric observations in order to clarify the nature of period variations more precisely. Eggen has also pointed out that a further study of these systems would yield much information about the evolution of binaries as well as being a proving ground for theories which might be applicable to more normal stars.

iv) Summary of Published Observations on the Three W Ursa Majoris Systems VW Cephi, 44i Bootes and W Ursa Majoris

VW Cephi

This short period variable was discovered by Schildt in 1926 (23). Since that time various observers have found the period to be changing. The following graph published in

a paper by Schmidt and Schrick (24) of observed minus computed times of minimum light over a period of about 30 years shows that the period was decreasing till about 1935 when it increased abruptly. The period then decreased slowly till about 1945 when it decreased abruptly. Subsequently, up to 1956 the period was decreasing slowly. The variations appear to be systematic.

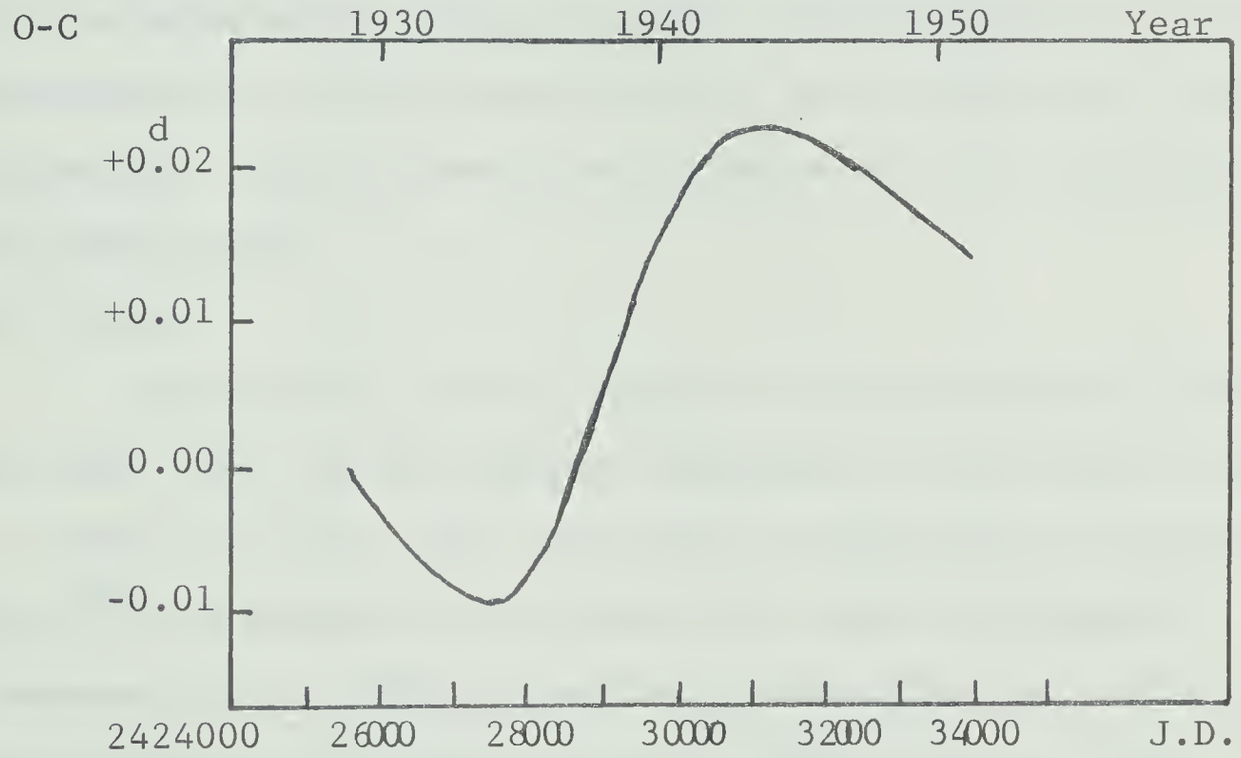

Figure 3.1 Observed minus computed times of minimum light for VW Cephi

To account for the variations in the relative heights of the maxima which had been seen by various observers and verified by themselves, Schmidt and Schrick proposed a model of the binary system in which additional gas in either of two states was present. In one state the gas was contained in the region

between the two stars, in the other state the gas surrounded both stars. In this latter state it was possible for gas to escape from the system in an axial region beyond the smaller star. They maintained that intrinsic changes could not cause the period variations since the changes appeared oscillatory. They also suggested that there might be a third body which accounted for the period variations as well as causing transitions between the two gas states. The possibility of the existence of a third body had first been stated by C. Payne Gaposchkin (25) .However, no evidence of such a body has yet been found.

44i Bootes

This short period variable was discovered by Schildt in 1926 (23) as the fainter component of the visual binary Σ 1909. At that time, the observed amplitude of eclipse was $0^m_.4$, at present it is about $0^m_.2$, since the brighter component of Σ 1909 is partially obscuring the variable in the course of its orbital motion. Eggen found in 1948 (22) that the distortions observed in the light curve were a real effect. He suggested that, within the limits of accuracy of the observations, it appeared possible that the double star system was a contact binary in which equalization of the masses was occuring via a gas stream which might account for the light curve irregularities. He also concluded that observed period variations were not entirely due to motion of the

visual orbit. He finally pointed out that more accurate light curves were needed to account for the deformation of maxima of the light curve and the intrinsic variation of period. In 1955 Binnendijk (26) suggested the system was near the limit of stability. The following graph of observed minus computed times of minimum light published by Binnendijk shows the nature of the period variations up to 1955.

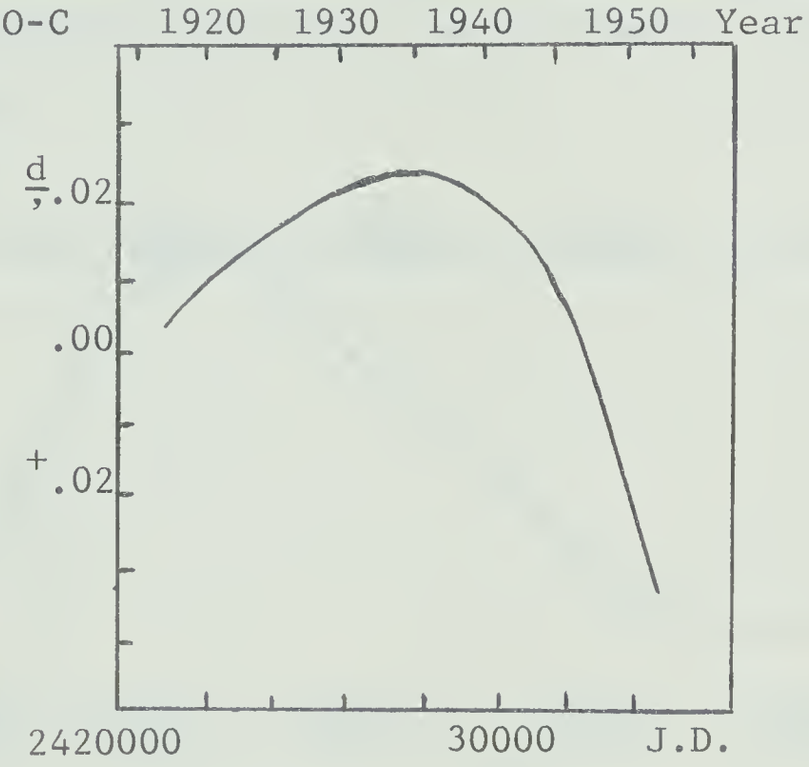

Figure 3.2 Observed minus computed times of minimum light for 44i Bootes

The graph shows that the period has been increasing since the system was first observed. The period changed abruptly by about .4 sec. in 1936. Since that time (up to 1954) the period has been increasing slowly.

W Ursa Majoris

This short period variable was discovered by Muller and Kempf in 1903 (27). Since that time observations of times of minima have revealed a variation of the period. The shapes and heights of the maxima have been seen to vary in an irregular manner. The nature of the variations in the period can be seen from the graph of observed minus computed times of minimum light published by Schmidt and Schrick in 1956 (15).

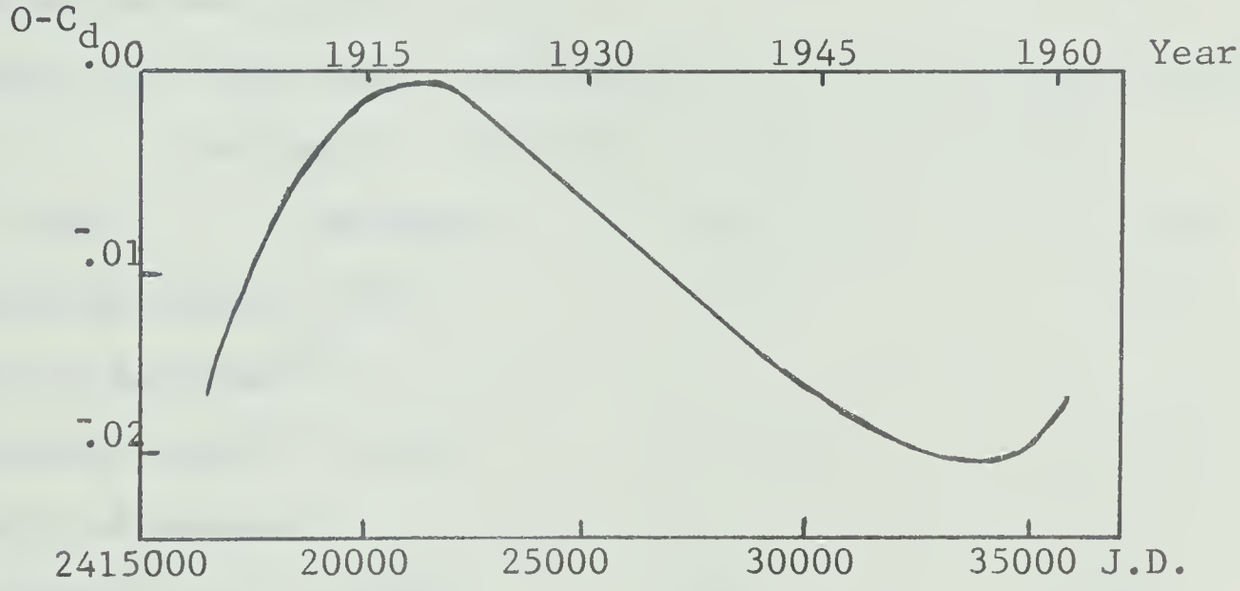

Figure 3.3 Observed minus computed times of minimum light for W Ursa Majoris

It is seen the period was almost constant from the time of discovery till about 1912 after which the period decreased fairly rapidly until about 1922. After remaining fairly constant until about 1941 the period again began to lengthen and has continued to do so ever since.

Huffer (28) had predicted that if the period variations are caused by a third body the period of variation should be greater than 30 years and the amplitude of the graph of times of minimum light should be > .01 days. The study of the system by Schmidt and Schrick suggested that the ejection of matter from the system was not the entire answer for the cause of period variations and consequently the effect of a third body must also be considered. In 1959 Chou (29) had indicated that it was still not possible to tell if the period variation was cyclic or not.

Table 3.1 Magnitudes and Elements of the Eclipsing Variables VW Cephi, 44i Bootes, and W Ursa Majoris

Star	VW Cephi	44i Bootes	W U Ma.
apparent magnitude at maximum(1)	$7^m.8$ +	$6^m.6$	$8^m.3$
spectral type(2)	K1+G6	G2 + F9	F8+F7
depth of primary minimum(3)	$0^m.35$	$0^m.42$ *	$0^m.60$
depth of secondary minimum(3)	$0^m.26$	$0^m.42$	$0^m.60$
type of primary eclipse(3)	annular partial	partial	partial
period (days)(3)	.2783	.2678	.3336
mass of primary component(2) (solar masses)	1.44	1.35	1.30

Star	VW Cephi	44i Bootes	W U Ma.
mass of secondary component[2] (solar masses)	.47	.68	.65
radius of primary component[2] (solar radii)	1.1	.98	1.11
radius of secondary component[2] (solar radii)	.62	.70	.79

Notes:

(1) - information from the catalogue of variable stars by Kukarkin (30).

(2) - information from tables prepared by Kopal and Shapely (31).

(3) - information from tables prepared by Payne Gaposchkin and Gaposchkin (32).

+ - stated magnitude of VW Cephi is the photoelectric magnitude, photographic magnitude are given for 44i Bootes and W Ursa Majoris.

* - the depth of the minima of 44i Bootes are $0^{m}.40$ when the components of the visual binary are both visible. When the brighter component of the visual binary obscures the fainter component of the visual binary (the eclipsing variable) the depth of minima can become less than $0^{m}.20$.

CHAPTER 4

THE OBSERVATIONS

The observed magnitude difference between the comparison and variable star in the blue and yellow colours and the times of observation in each of these colours (in heliocentric Julian days) are tabulated in Tables 4.1 - 4.3 for each of the W Ursa Majoris Systems. The letter o indicates magnitude differences determined from measurements made by the observing assistant, while the letter r indicates magnitude differences determined from measurements made with the digital recorder. The observations of VW Cephi on three nights are shown (superimposed) in Graph 4.1. The magnitude differences are plotted against the phase ϕ, where $\phi = (t - T_o)/P$ (T_o = time of minimum light). The observations of 44i Bootes are plotted individually in Graphs 4.2, 4.3 and 4.4. In this case the magnitude differences are plotted against the heliocentric Julian date. The observations of W Ursa Majoris on two nights are superimposed in Graph 4.5 where the magnitude differences are plotted against the phase ϕ.

The magnitude differences determined from measurements made by the observing assistant are estimated to be accurate to $\pm\ 0^m.025$ while the magnitude differences determined from measurements made with the digital recorder are estimated

to be accurate to $\pm$ $^{m}0.015$. The individual times of observation were recorded to $\pm$ 3 secs.

It is seen from Graph 4.1 the blue and yellow light curves, obtained for VW Cephi by superimposing the observations of 3 nights, are well defined. The typical departure of individual points from the mean light curves is less than $0^{m}.03$. The observations in blue on March 20 depart considerably from the mean light curve for $\phi > .06$, similarly, the observations in yellow on February 27 depart considerably from the mean light curve for $\phi > .08$. In both cases this is attributed to personal errors in brightness measurements. Due to the deformation of the blue light curve on March 20, attributed to personal errors, the observations in this colour were not used to calculate the times of minimum light on that night.

On the morning of March 7, 1968 (JD2439922.5) an irregularity was observed in the light curve of 44i Bootes (Graph 4.2) which preceded primary minimum. At first it was thought the irregularity might be due to inaccuracies of measurement. However, after it was noted that the distortion appeared to be similar in both colours, it was decided the irregularity was probably real. The irregularity appeared to be a depression in the light curve, which began shortly after

maximum light, and which lasted for approximately ½ hour. Such irregularities have been seen by other observers (22). As has been suggested in Chapter 3, this sort of deformity is probably caused by a physical change in the gas clouds between the component stars. From the light curve it appears that the depression has a larger amplitude in the visual colour than in the blue colour. However, due to the limitations in the accuracy of the magnitude measurements, this cannot be stated with certainty. It can also be noted that the magnitudes at primary minimum, which were observed on two different nights, differ by about $0^m_.02$ in both colours. This behavior has previously been noted by Binnendijk (26), who has suggested the magnitude variation might occur because of slight variability in the brightest component of the three star system (see page 42).

The blue and yellow light curves, obtained for W Ursa Majoris by superimposing the observations of 2 nights, are well defined. In eclipse the typical departure of individual points is less than $0^m_.02$. Outside eclipse near the maxima scatter of points is considerably greater, typically $0^m_.05$. The scatter of points near maximum light is characteristic of W Ursa Majoris and is considered to be due to physical changes in the gas clouds surrounding the component stars.

Table 4.1 Observations of VW Cephi

hel.J.D.°	$(m_c-m_v)_b$	hel.J.D.°	$(m_c-m_v)_v$
2439914.000+		2439914.000+	
.7426	1.044	.7427	.728
.7452	1.033	.7454	.710
.7476	1.016	.7477	.760
.7502	1.024	.7503	.637
.7523	.993	.7524	.655
.7539	.988	.7540	.656
.7560	.958	.7562	.649
.7575	.954	.7571	.624
.7600	.945	.7601	.599
.7634	.901	.7635	.579
.7662	.855	.7663	.550
.7678	.847	.7679	.546
.7732	.823	.7735	.472
.7773	.797	.7774	.418
.7789	.725	.7790	.409
.7822	.707	.7823	.399
.7839	.711	.7841	.404
.7858	.716	.7860	.434
.7878	.725	.7879	.444
.7898	.748	.7900	.444
.7928	.770	.7929	.457

hel.J.D.°	$(m_c-m_v)_b$	hel.J.D.°	$(m_c-m_v)_v$
2439914.000+		2439914.000+	
.7949	.789	.7950	.501
.7988	.823	.7990	.545
.8018	.879	.8021	.561
.8050	.910	.8051	.567
.8071	.937	.8072	.630
.8108	.973	.8109	.630
.8144	.980	.8146	.646
.8166	1.009	.8168	.663
hel.J.D.°	$(m_c-m_v)_b$	hel.J.D.°	$(m_c-m_v)_v$
2439936.000+		2439936.000+	
.7096	1.145	.7098	.805
.7113	1.115	.7115	.804
.7136	1.100	.7138	.766
.7160	1.093	.7162	.746
.7221	1.080	.7223	.740
.7245	1.065	.7247	.740
.7263	1.050	.7265	.726
.7286	1.055	.7288	.720
.7305	1.039	.7307	.701
.7330	1.019	.7332	.688
.7351	1.003	.7353	.661
.7372	.979	.7374	.661
.7398	.954	.7400	.654

hel.J.D.°	$(m_c-m_v)_b$	hel.J.D.°	$(m_c-m_v)_v$
2439936.000+		2439936.000+	
.7420	.954	.7422	.633
.7452	.937	.7454	.604
.7523	.849	.7525	.563
.7565	.811	.7567	.521
.7584	.792	.7586	.491
.7613	.752	.7614	.432
.7634	.753	.7636	.453
.7655	.732	.7656	.436
.7678	.712	.7680	.410
.7709	.712	.7711	.407
.7744	.743	.7746	.423
.7770	.753	.7772	.466
.7814	.811	.7816	.486
.7819	.830	.7821	.501
.7848	.849	.7850	.529
.7863	.867	.7865	.559
.7890	.920	.7892	.588
.7916	.954	.7918	.624
.7945	.976	.7947	.647
.7969	.995	.7971	.604
.7987	1.034	.7990	.688
.8000	1.047	.8010	.707
.8024	1.039	.8029	.723

hel.J.D.^{r} 2439949.000+	$(m_c-m_v)_b$	hel.J.D.^{r} 2439949.000+	$(m_c-m_v)_v$
.7940	1.127	.7942	.773
.7998	1.114	.8000	.819
.8039	1.078	.8042	.759
.8062	1.078	.8065	.770
.8089	1.073	.8092	.735
.8116	1.066	.8119	.717
.8145	1.042	.8148	.710
.8174	1.021	.8176	.681
.8198	1.009	.8201	.668
.8225	.968	.8228	.616
.8251	.965	.8253	.627
.8274	.966	.8278	.623
.8299	.960	.8302	.600
.8330	.858	.8333	.574
.8366	.840	.8369	.527
.8394	.815	.8397	.495
.8420	.773	.8423	.468
.8441	.729	.8444	.418
.8494	.732	.8496	.428
.8522	.717	.8524	.402
.8565	.717	.8568	.434
.8596	.756	.8599	.461
.8624	.811	.8627	.501

hel.J.D.^{r} 2439949.000+	$(m_c-m_v)_b$	hel.J.D.^{r} 2439949.000+	$(m_c-m_v)_v$
.8647	.846	.8650	.510
.8673	.847	.8675	.531
.8700	.882	.8702	.576
.8727	.910	.8730	.599
.8759	.922	.8762	.617
.8788	.969	.8791	.662
.8811	.993	.8814	.688

Table 4.2 Observations of 44i Bootes

hel.J.D.° 2439922.000+	$(m_c-m_v)_b$	hel.J.D.° 2439922.000+	$(m_c-m_v)_v$
.8162	.701	.8164	.883
.8213	.709	.8215	.872
.8244	.745	.8247	.872
.8276	.735	.8277	.882
.8338	.744	.8341	.910
.8370	.752	.8372	.909
.8403	.760	.8407	.919
.8438	.768	.8440	.919
.8473	.775	.8478	.928
.8532	.775	.8536	.927
.8561	.775	.8564	.936
.8616	.774	.8619	.918

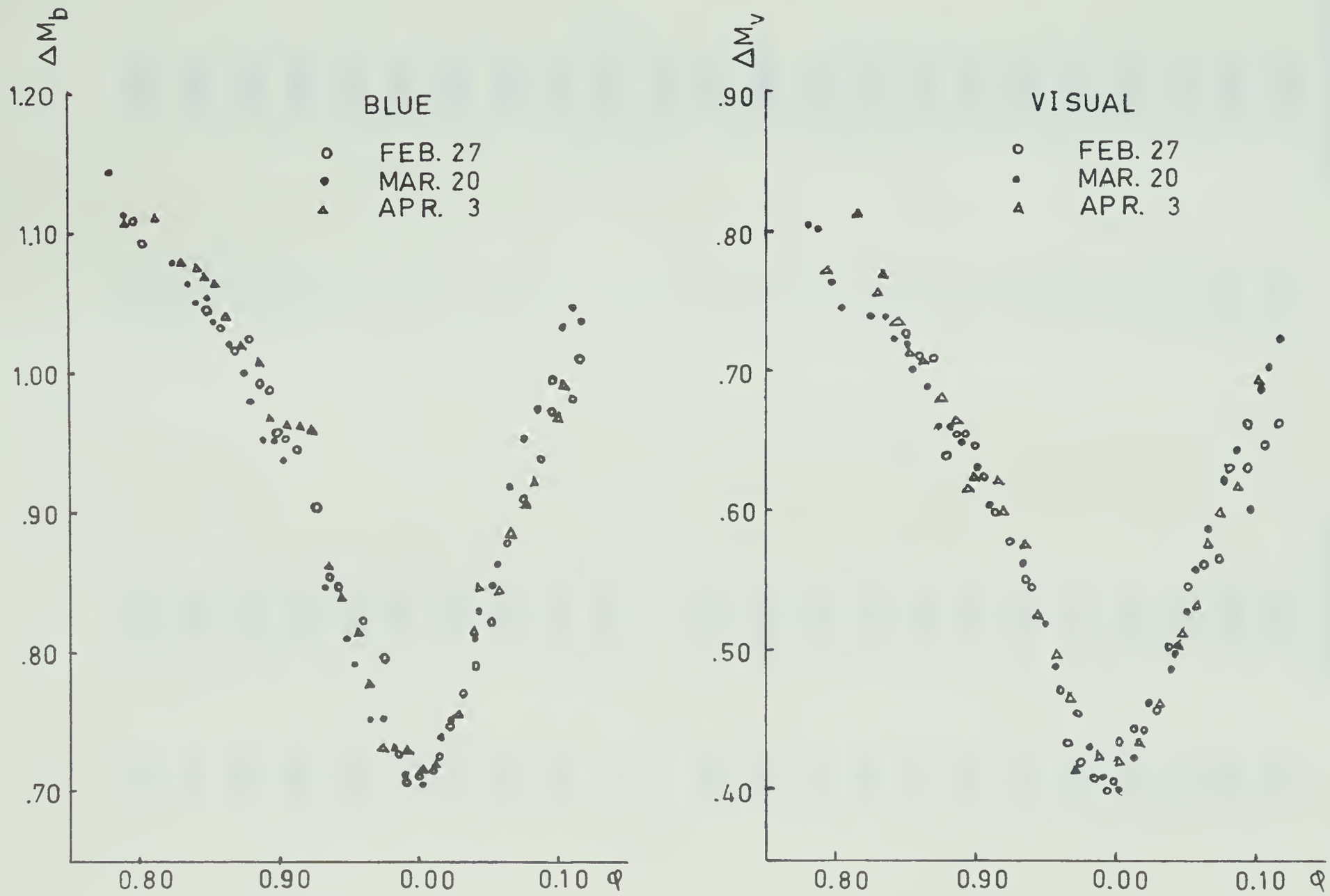

GRAPH 4.1 PRIMARY MINIMUM OF VW CEPHI

hel.J.D.° 2439922.000+	$(m_c-m_v)_b$	hel.J.D.° 2439922.000+	$(m_c-m_v)_v$
.8653	.758	.8655	.917
.8684	.750	.8686	.914
.8719	.750	.8721	.886
.8748	.740	.8753	.886
.8784	.740	.8787	.876
.8822	.740	.8826	.876
.8860	.740	.8862	.876
.8887	.730	.8889	.878
.8911	.722	.8916	.887
.8942	.713	.8944	.878
.8998	.695	.9000	.837
.9029	.669	.9034	.828
.9108	.651		
.9129	.623	.9131	.776
.9154	.613	.9156	.766
.9197	.588	.9200	.765
.9215	.595	.9217	.754
.9241	.585	.9243	.754
.9270	.594	.9275	.754
.9301	.603	.9303	.754
.9331	.623	.9333	.765
.9355	.623	.9357	.765
.9387	.632	.9389	.785

hel.J.D.° 2439922.000+	$(m_c-m_v)_b$	hel.J.D.° 2439922.000+	$(m_c-m_v)_v$
.9417	.649	.9418	.805
.9435	.649	.9436	.805
.9461	.667	.9463	.815
.9481	.667	.9484	.837
.9510	.685	.9522	.835
.9545	.693	.9547	.852
.9571	.702	.9573	.864
.9607	.702	.9608	.852
.9628	.709	.9643	.852
.9675	.718	.9677	.882
.9711	.726	.9713	.882
.9780	.735	.9785	.892
hel.J.D.° 2439935.000+	$(m_c-m_v)_b$	hel.J.D.° 2439935.000+	$(m_c-m_v)_v$
.8565	.755	.8567	.923
.8600	.760	.8601	.922
.8626	.765	.8627	.923
.8660	.757	.8665	.913
.8746	.746	.8751	.906
.8778	.734	.8780	.899
.8806	.726	.8808	.885
.8841	.732	.8844	.883
.8869	.732	.8871	.871

hel.J.D.° 2439935.000+	$(m_c-m_v)_b$	hel.J.D.° 2439935.000+	$(m_c-m_v)_v$
.8900	.726	.8902	.864
.8936	.706	.8938	.853
.9861	.708	.8963	.843
.8991	.698	.8998	.827
.9025	.695	.9027	.821
.9058	.679	.9060	.820
.9082	.657	.9084	.810
.9117	.656	.9119	.793
.9149	.666	.9152	.801
.9186	.663	.9188	.810
.9218	.670	.9221	.820
.9251	.674	.9253	.831
.9282	.689	.9284	.841
.9329	.709	.9331	.803
.9366	.719	.9368	.864
.9421	.734	.9423	.886
.9461	.740	.9463	.899
.9512	.750	.9514	.909
.9546	.747	.9548	.916
.9574	.756	.9576	.909
.9609	.769	.9611	.925
.9642	.763	.9646	.920

hel.J.D.^{r} 2439952.000+	$(m_c-m_v)_b$	hel.J.D.^{r} 2439952.000+	$(m_c-m_v)_v$
.8546	.722	.8549	1.043
.8648	.764	.8651	.919
.8681	.754	.8684	.917
.8719	.757	.8723	.916
.8759	.748	.8762	.905
.8780	.744	.8786	.899
.8820	.731	.8823	.896
.8854	.729	.8859	.877
.8881	.726	.8885	.870
.8908	.721	.8913	.873
.8936	.702	.8939	.865
.8966	.703	.8969	.853
.8993	.693	.8996	.840
.9023	.670	.9026	.819
.9050	.657	.9053	.807
.9079	.638	.9082	.793
.9105	.627	.9108	.789
.9131	.617	.9134	.776
.9157	.606	.9160	.762
.9183	.612	.9188	.767
.9218	.610	.9222	.770
.9331	.644	.9338	.800
.9374	.667	.9377	.816

hel.J.D.^{r} 2439952.000+	$(m_c-m_v)_b$	hel.J.D.^{r} 2439952.000+	$(m_c-m_v)_v$
.9399	.670	.9403	.804
.9431	.678	.9434	.836
.9455	.692	.9458	.853
.9482	.706	.9485	.867
.9508	.705	.9511	.870
.9533	.706	.9536	.874
.9567	.722	.9570	.883
.9592	.733	.9595	.880
.9631	.736	.9634	.893
.9656	.738	.9659	.880
.9713	.750	.9720	.908
.9757	.765	.9762	.907

GRAPH 4.2 44i BOOTES March 7th 1968

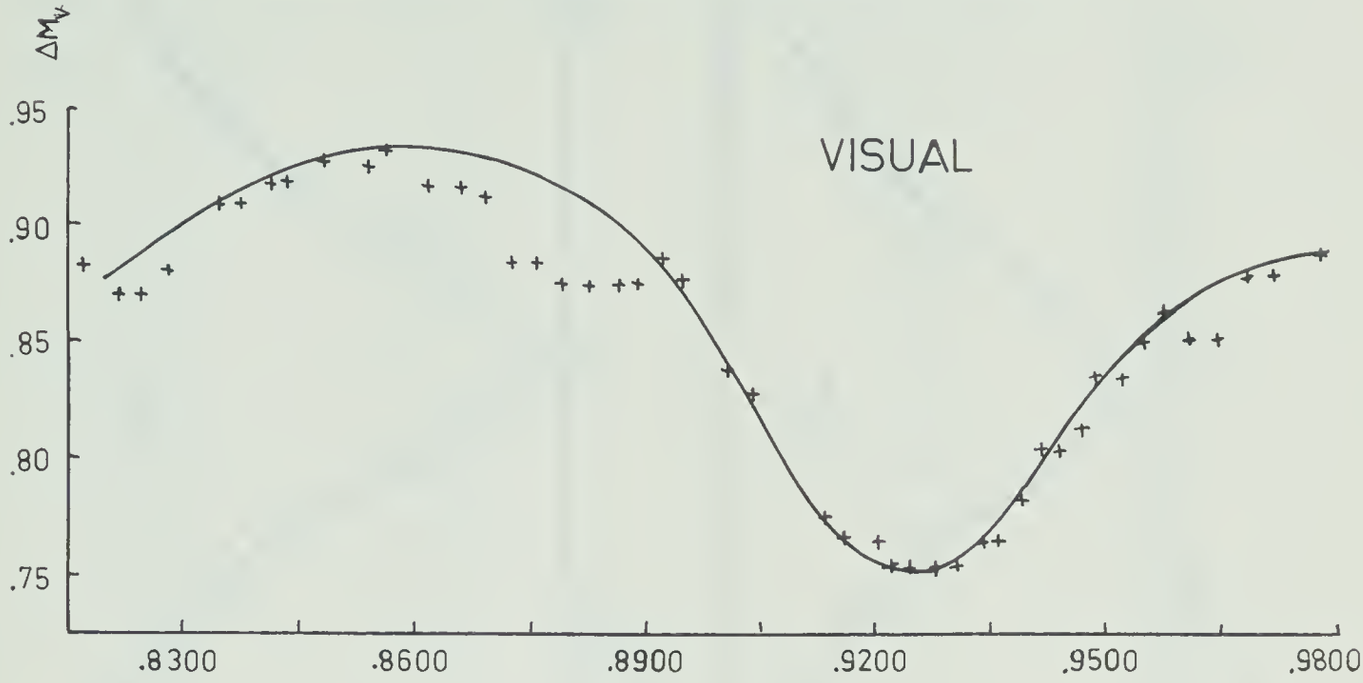

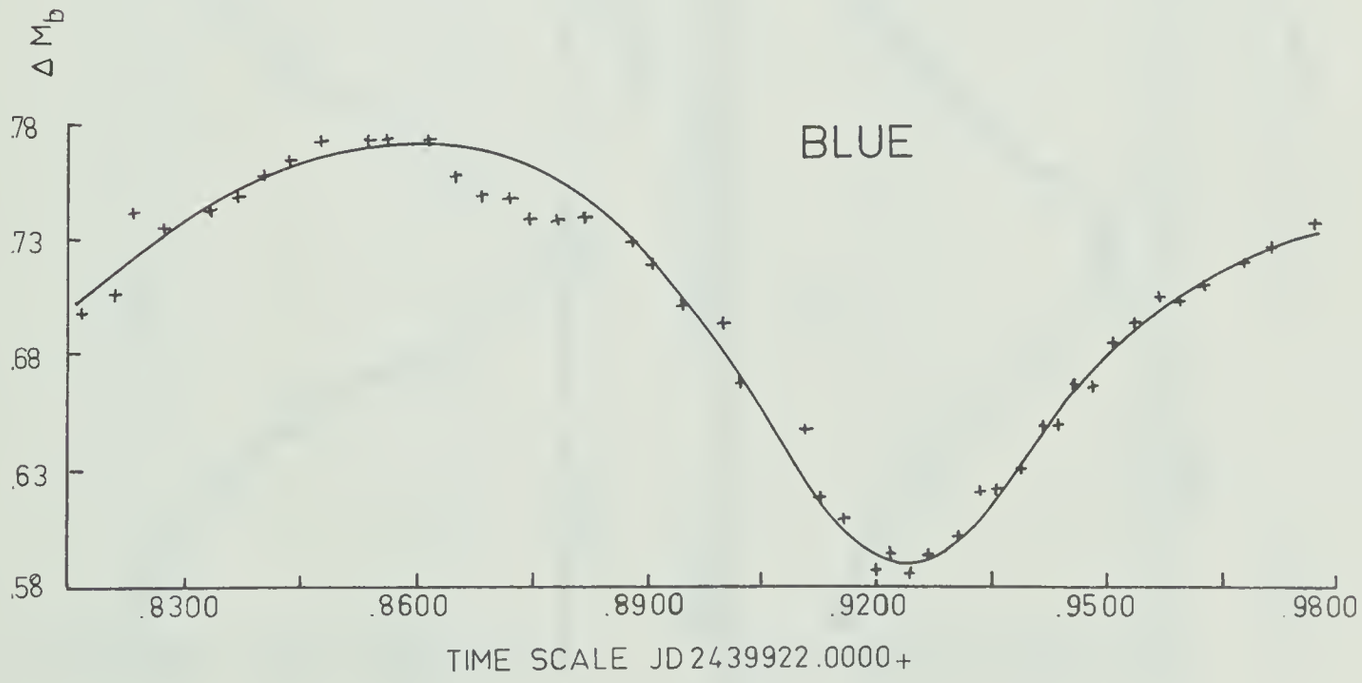

TIME SCALE JD 2439922.0000+

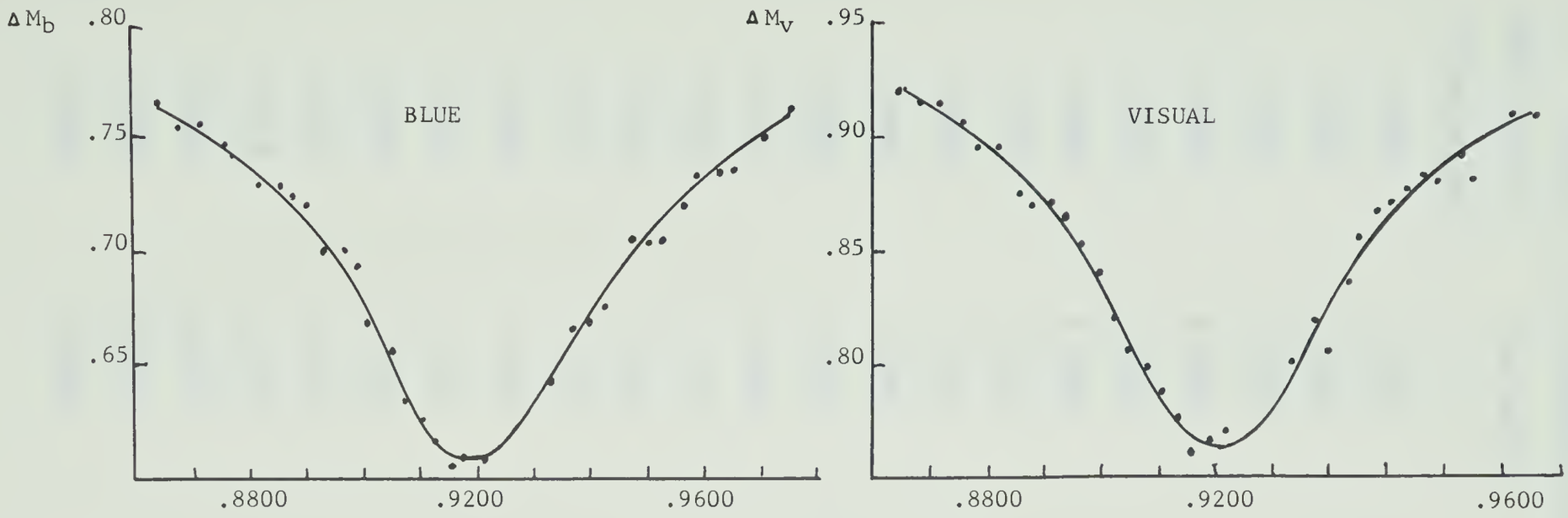

GRAPH 4.3 PRIMARY MINIMUM OF 44i BOOTES

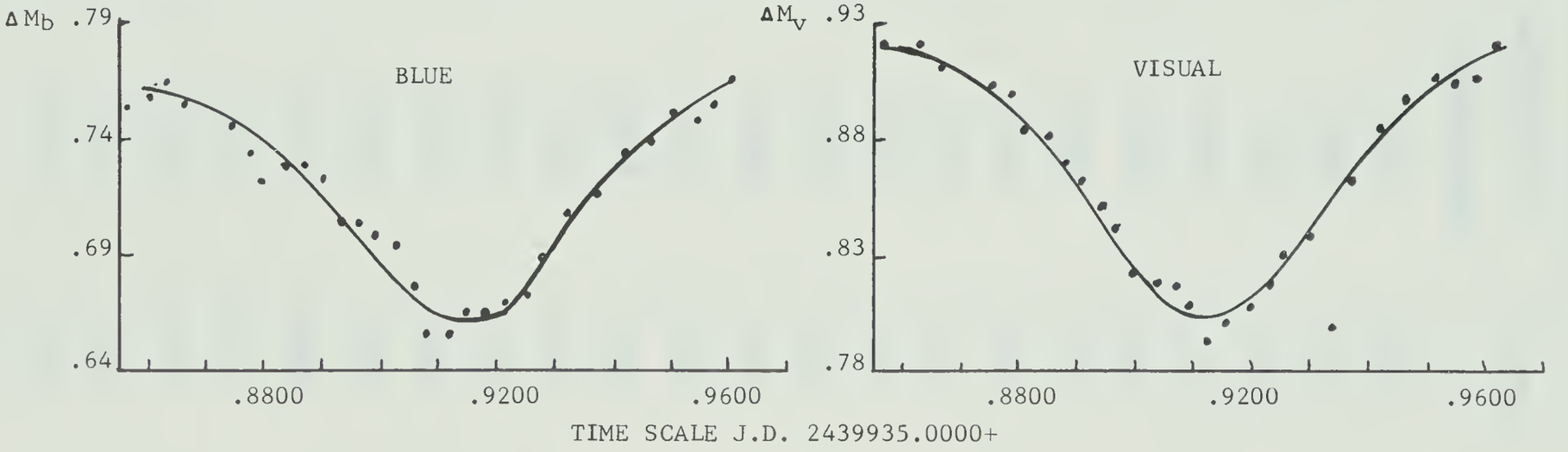

GRAPH 4.4 SECONDARY MINIMUM OF 44i BOOTES

Table 4.3 Observations of W Ursa Majoris

hel.J.D.^{r} 2439959.000+	$(m_c-m_v)_b$	hel.J.D.^{r} 2439959.000+	$(m_c-m_v)_v$
.6697	1.333	.6699	1.140
.6721	1.367	.6724	1.111
.6746	1.385	.6749	1.133
.6798	1.353	.6801	1.128
.6828	1.381	.6830	1.161
.6858	1.381	.6860	1.154
.6882	1.377	.6885	1.143
.6914	1.382	.6923	1.145
.6949	1.397	.6951	1.162
.6985	1.391	.6990	1.148
.7017	1.383	.7020	1.183
.7049	1.377	.7052	1.170
.7075	1.356	.7078	1.126
.7116	1.354	.7119	1.122
.7144	1.341	.7147	1.116
.7170	1.334	.7173	1.200
.7195	1.328	.7198	1.098
.7224	1.304	.7227	1.096
.7252	1.293	.7255	1.077
.7281	1.277	.7284	1.057
.7308	1.259	.7310	1.060
.7334	1.249	.7337	1.051

hel.J.D.^{r} 2439959.000+	$(m_c-m_v)_b$	hel.J.D.^{r} 2439959.000+	$(m_c-m_v)_v$
.7363	1.235	.7366	1.033
.7394	1.220	.7397	1.016
.7422	1.199	.7425	.960
.7452	1.145	.7455	.913
.7481	1.097	.7483	.913
.7511	1.048	.7514	.932
.7524	1.112	.7527	.851
.7537	1.018	.7540	.777
.7569	.945	.7572	.724
.7604	.887	.7607	.691
.7637	.800	.7640	.616
.7672	.716	.7675	.563
.7711	.666	.7714	.500
.7743	.674	.7746	.494
.7771	.666	.7774	.463
.7809	.656	.7812	.475
.7841	.672	.7844	.500
.7870	.680	.7873	.543
.7908	.771	.7911	.613
.7943	.860	.7945	.697
.7976	.949	.7979	.791
.8009	1.012	.8012	.818
.8040	1.057	.8043	.870

hel.J.D.^{r}	$(m_c-m_v)_b$	hel.J.D.^{r}	$(m_v-m_v)_v$
2439959.000+		2439959.000+	
.8069	1.100	.8072	.889
.8110	1.182	.8114	.960
.8135	1.227	.8138	.999
.8175	1.247	.8178	1.016
hel.J.D.^{r}	$(m_c-m_v)_b$	hel.J.D.^{r}	$(m_v-m_v)_v$
2439967.000+		2439967.000+	
.7080	1.399	.7083	1.162
.7104	1.408	.7107	1.169
.7128	1.415	.7131	1.162
.7154	1.388	.7156	1.139
.7179	1.373	.7182	1.146
.7204	1.353	.7206	1.147
.7241	1.383	.7244	1.139
.7267	1.335	.7269	1.141
.7296	1.358	.7299	1.136
.7324	1.317	.7327	1.093
.7365	1.312	.7368	1.078
.7399	1.285	.7400	1.086
.7426	1.276	.7428	1.044
.7457	1.243	.7460	1.014
.7501	1.229	.7504	.974
.7532	1.185	.7545	.943
.7562	1.133	.7564	.924

hel.J.D.^{r} 2439967.000+	$(m_c-m_v)_b$	hel.J.D.^{r} 2439967.000+	$(m_v-m_v)_v$
.7594	1.085	.7602	.863
.7619	1.052	.7620	.804
.7646	.974	.7649	.769
.7675	.939	.7677	.740
.7701	.867	.7704	.697
.7729	.818	.7732	.601
.7758	.777	.7761	.563
.7787	.728	.7789	.527
.7816	.649	.7819	.499
.7846	.677	.7849	.486
.7875	.672	.7878	.478
.7900	.705	.7903	.500
.7923	.667	.7926	.486
.7955	.709	.7957	.508
.7982	.778	.7985	.527
.8004	.775	.8007	.580
.8036	.846	.8038	.669
.8058	.894	.8060	.713
.8083	.978	.8086	.759
.8107	1.043	.8109	.783
.8157	1.070	.8159	.840
.8164	1.117	.8167	.890
.8193	1.144	.8196	.934

hel.J.D.^{r} 2439967.000+	$(m_c-m_v)_b$	hel.J.D.^{r} 2439967.000+	$(m_v-m_v)_v$
.8219	1.195	.8222	.985
.8256	1.238	.8259	.988
.8280	1.256	.8283	1.007
.8310	1.243	.8313	1.036
.8340	1.275	.8343	1.051
.8371	1.310	.8374	1.056
.8407	1.321	.8410	1.070
.8442	1.336	.8445	1.111
.8471	1.339	.8474	1.120
.8500	1.362	.8502	1.121
.8521	1.345	.8524	1.115
.8549	1.365	.8551	1.148

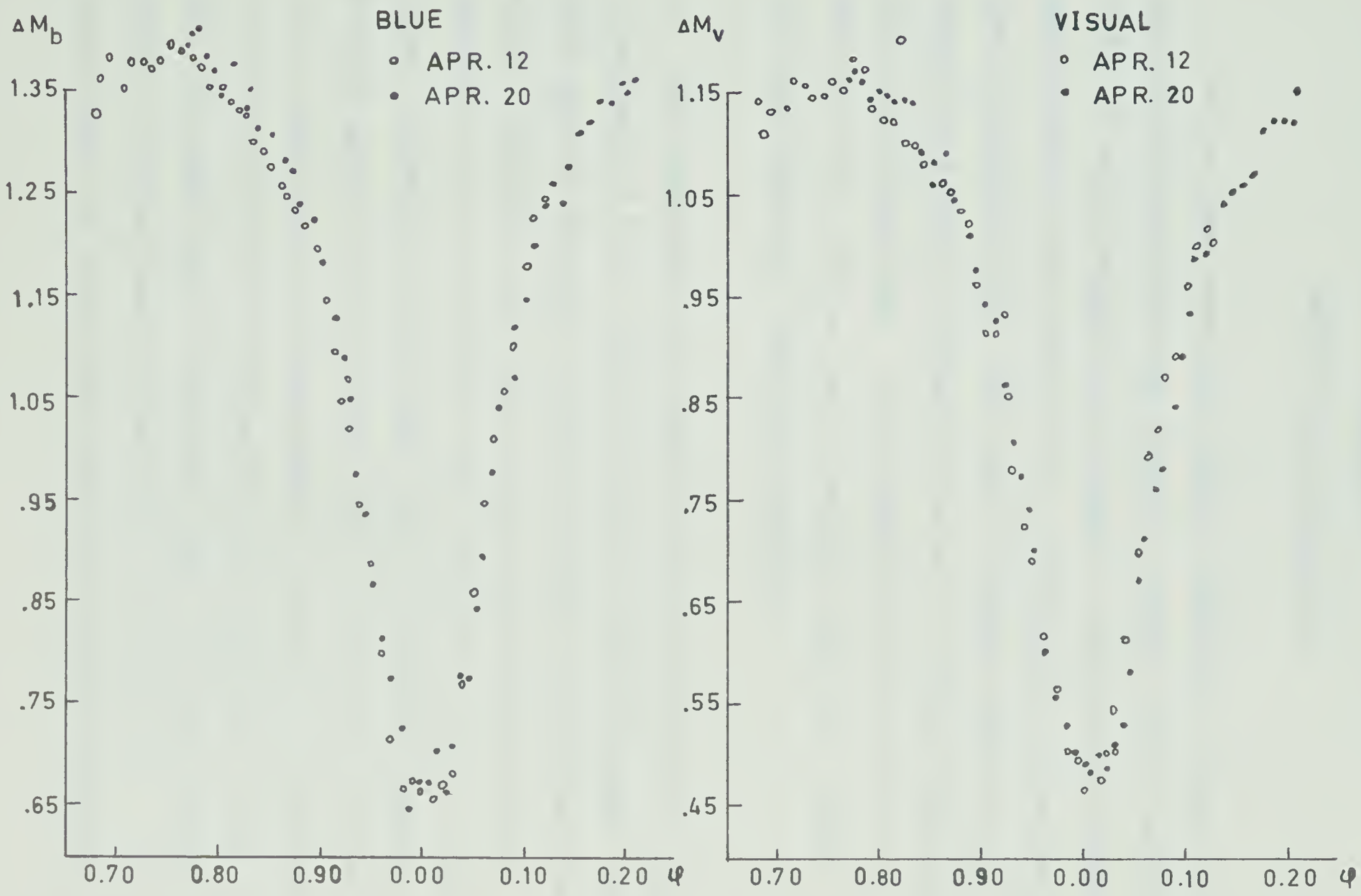

GRAPH 4.5 PRIMARY MINIMUM OF W URSA MAJORIS

CHAPTER 5

RESULTS AND DISCUSSION

As has been mentioned before, individual values for the time of minimum light were found by forming chords joining points of equal brightness on opposite sides of the light curve such that the midpoint of a chord gave a value for the time of minimum light. The time of minimum light in each colour was taken as the mean value of all these individual times of minimum light. The standard deviation of the individual values of the time of minimum light for a given light curve was typically $^{d}.0003$ (30 seconds).

The blue and visual light curves obtained for VW Cephi on February 27 (J.D. 2439914.5+) gave times of minimum light which were in agreement within 40 seconds. The given time of minimum light for this night is the mean value of all the individual times of minimum light obtained from both light curves. On March 20 the light curves of both 44i Bootes and VW Cephi gave times of minimum light in the blue and visual colours which were in disagreement by more than 1½ minutes. It was found for both systems that the individual values of time of minimum light on the blue light curve were widely discordant, whereas those on the visual curve were not. This indicated that the blue light curves were poorly formed due to

either personal errors in the brightness measurements or systematic errors due to large changes in atmospheric transparency. Consequently, the times of minimum light on these nights were taken to be the times of minimum light as determined from the visual light curves. On all other nights the times of minimum light deduced from the light curves in the blue and visual colours were in agreement within 20 seconds. For these nights, the given time of minimum light is the average value of the individual times of minimum light obtained from both curves.

Because of the systematic and personal errors in the magnitude measurements, the light curves are not completely accurate records of the magnitude changes of the eclipsing variables, hence the determined times of minimum light are not without some error. The error in determination of the times of minimum light is estimated to be $\pm$ $^{d}.0005$ ($\pm$ 44 seconds).

The observed times of minimum light are as follows:

VW Cephi

Primary Minimum

hel. J.D. 2439914.7838

hel. J.D. 2439936.7707

hel. J.D. 2439949.8514

44i Bootes

Primary Minimum

hel. J.D. 2439922.9249

hel. J.D. 2439952.9211

Secondary Minimum

hel. J.D. 2439935.9133

W Ursa Majoris

Primary Minimum

hel. J.D. 2439959.7769

hel. J.D. 2439967.7854

The period changes are discussed in the following paragraphs.

i) VW Cephi

The observed times of minimum light up to 1955 have been tabulated in a paper by Schmidt and Schrick (24). The times of minimum light found by Schmidt and Schrick, Rakosch (33) and from the present project are listed in Table 5.1. The differences between the observed times of minimum light and the predicted times of minimum light computed from the element: Primary Minimum = 2424658.759 + $^{d}.27831993E$ are listed in the (O-C) column. The above element is the constant part of an element given by Huffer (34).

Table 5.1 Times of Minimum Light of VW Cephi

J.D.	Authority	(O-C)
2434768.464	Schmidt - Schrick	+.012
37780.433	Schmidt - Schrick	.013
36857.5157	Rakosch	-.0058
36858.3495	Rakosch	.0070
36859.4630	Rakosch	.0068
39914.7863	Brown	.0822
39936.7707	Brown	.0825
39949.8514	Brown	.0829

Graph 5.1 consists of the graph of observed minus computed times of minimum light prepared by Schmidt and Schrick plus an extension of this graph (indicated by the dashed portion of the graph) through the times of minimum light obtained by Rakosch and from the present project.

The continued decrease in the slope of the O-C graph indicates that the period is still continuing to decrease at this time. An estimation of the slope of the graph in 1960 and 1968 reveals that a decrease in period of the order of one second has occured in the last eight years. The continuous decrease in the period since 1940 would seem to suggest that the period changes are caused by internal changes in the binary system. However, the graph of observed minus computed times of minimum light still does not give a definite indication as to whether period changes are caused

GRAPH 5.1 OBSERVED MINUS COMPUTED TIMES OF MINIMUM LIGHT OF V W CEPHI (1968)

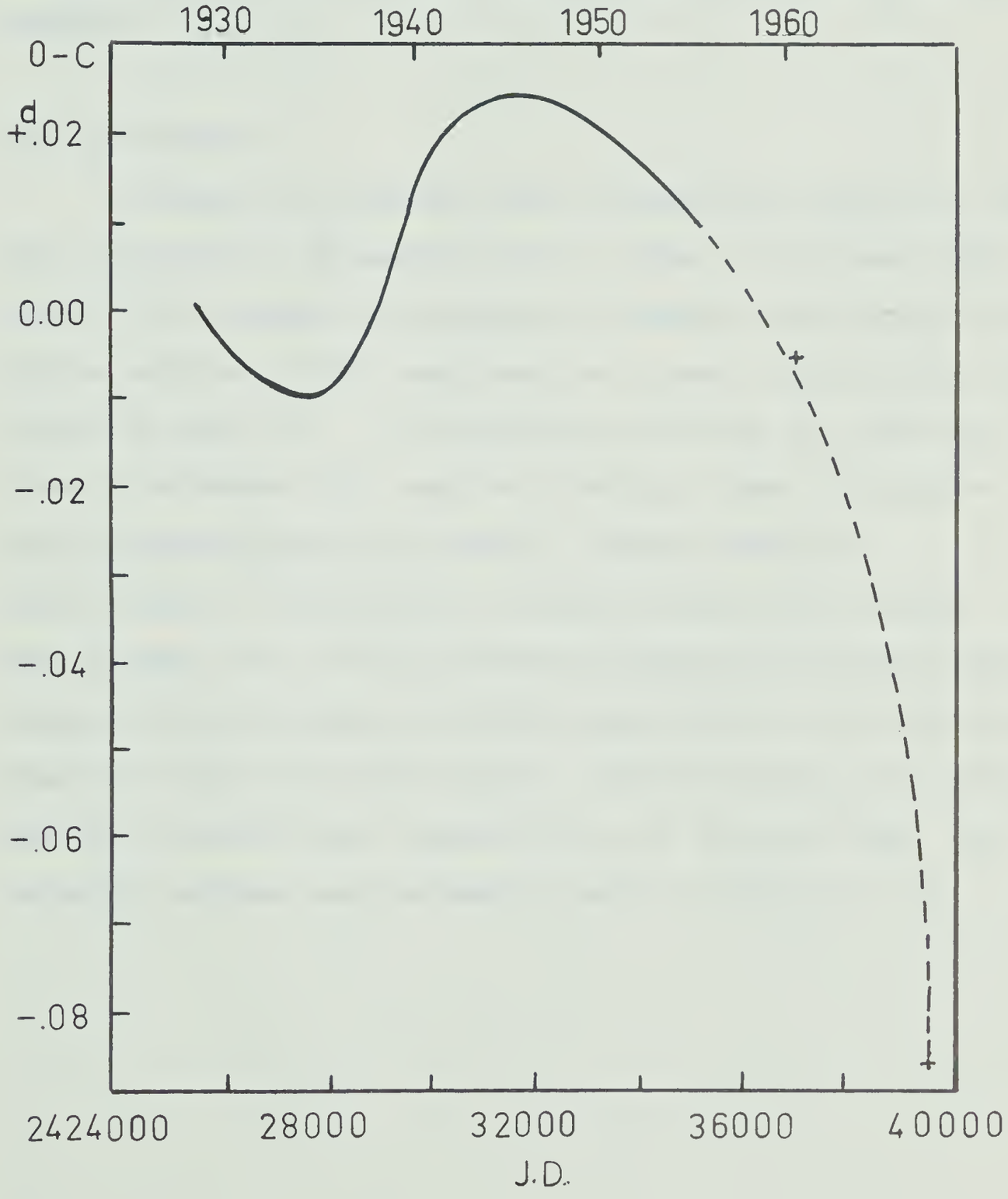

by intrinsic changes in the binary system, by third body perturbations, or by a combination of these. Therefore, observations of times of minimum light will be required for many years to come in order to determine the nature of period changes.

ii) 44i Bootes

A summary of observed times of minimum light up to 1955 has been given by Binnendijk (26). Times of minimum light since 1956, obtained from papers by Schmidt and Schrick (35), Wehlau and Leung (36), and from the present observations are listed in Table 5.2. The difference between the observed times of minimum light and the predicted times of minimum light computed from the element: Primary Minimum = 2421113.2588 + ^{d}.26780832E is listed in the (O-C) column. This element was used by the above mentioned observers for the purpose of calculating the differences between observed and computed times of minimum light. For the purpose of calculating the observed minus computed time of minimum light, the secondary minimum was assumed to occur at phase ϕ = .5.

Table 5.2 Times of Minimum Light of 44i Bootes

J.D.	Authority	(O-C)
2434876.4988	Schmidt - Schrick	+.0348
35341.4252	Schmidt - Schrick	.0460
35601.4725	Schmidt - Schrick	.0514
35694.4010	Schmidt - Schrick	.0504
35927.3997	Schmidt - Schrick	.0559
35932.4875	Schmidt - Schrick	.0553
37443.7660	Wehlau - Leung	.0988
37449.6577	Wehlau - Leung	.0987
37472.6889	Wehlau - Leung	.0988
39922.9249	Brown	.1487
39935.9133	Brown	.1481
39952.9211	Brown	.1506

Graph 5.2 consists of the graph of observed minus computed times of minimum light obtained by Binnendijk (26) plus an extension of this graph (indicated by the dashed portion of the graph) through the times of minimum light obtained by Schmidt and Schrick, Wehlau and Leung and from the present project.

The large variation of the observed minus computed times of minimum light is due mainly to the orbital motion of the visual binary. The decreasing slope of the graph at the present time indicates the motion of the eclipsing binary is now towards the earth. The graph appears to be continuous which indicates that the slow increase in period due to

GRAPH 5.2 OBSERVED MINUS COMPUTED TIMES
OF MINIMUM LIGHT OF 44i BOOTES(1968)

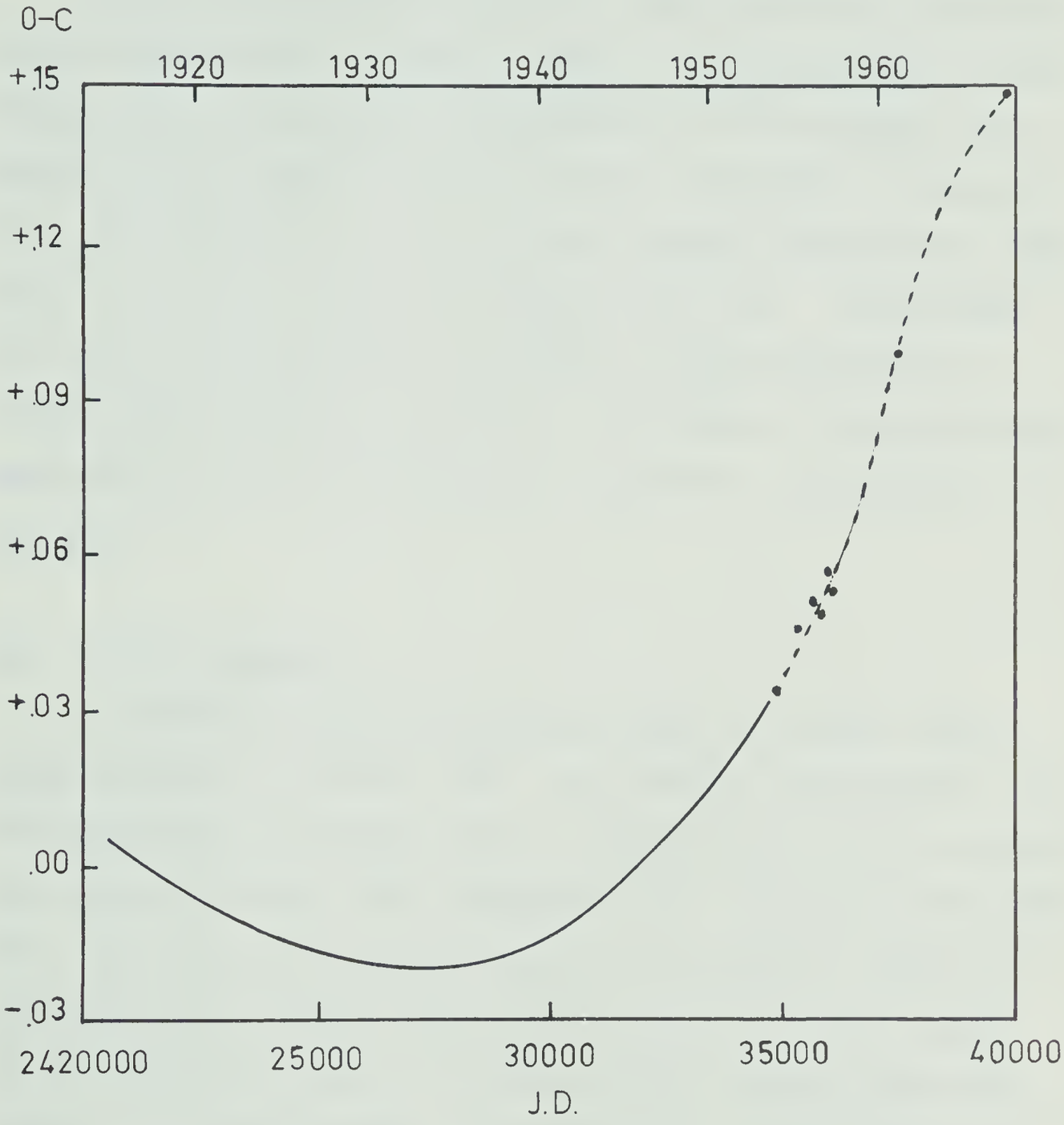

intrinsic changes in the eclipsing binary is still continuing.

As has been mentioned before a depression was observed in the light curve on March 7, 1968. The depression is most likely due to the partial obscuration of the secondary component by gas ejected from the primary component of the system. The ejection of gas from the primary component has been seen to occur at irregular intervals (22, 35). This being the case, the differences in depths of the depression in visual and blue colours would be attributed to the wavelength dependence of the scattering and absorption coefficients of the gas.

iii) W Ursa Majoris

A record of times of minimum light up to 1956 can be found in papers by Huffer (28), and Schmidt and Schrick (15). Selected times of minimum light, observed since 1956, obtained from papers by Chou (29), Bookmeyer (37), Blitzstein and Chou (38), and from the present project, are listed in Table 5.3. The difference between the observed times of minimum light and the predicted times of minimum light computed from the element: Primary Minimum = 2421856.9401 + .333637665E is listed in the (O-C) column. This element was used by Schmidt and Schrick for the purpose of calculating observed minus computed times of minimum light.

Table 5.3 Times of Minimum Light of W Ursa Majoris

J.D.	Authority	(O-C)
2436611.7163	Chou	-.0159
36634.7367	Bookmeyer	.0165
36635.7377	Bookmeyer	.0165
36698.7090	Bookmeyer	.0155
37369.7412	Blitzstein - Chou	.0158
37376.7477	Blitzstein - Chou	.0156
37379.7503	Blitzstein - Chou	.0158
39959.7769	Brown	.0092
39967.7854	Brown	.0081

Graph 5.3 consists of the graph of observed minus computed times of minimum light obtained by Schmidt and Schrick plus an extension of this graph (indicated by the dashed segment of the graph) through the times of minimum light listed in Table 5.3.

A continuing increase in the period is indicated by the fact that the slope of the graph is still increasing at this time. Furthermore, if one takes into account the fact that the segment of the O-C graph from 1900 to 1912 is probably not too well formed due to the relatively poor determination of the times of minimum light during this period, the slope of the graph appears to have comparible values in the periods 1900 - 1912 and 1960 - 1968. Thus there is an indication that the period variation is cyclic which would be in

GRAPH 5.3 OBSERVED MINUS COMPUTED TIMES OF MINIMUM LIGHT OF W URSA MAJORIS(1968)

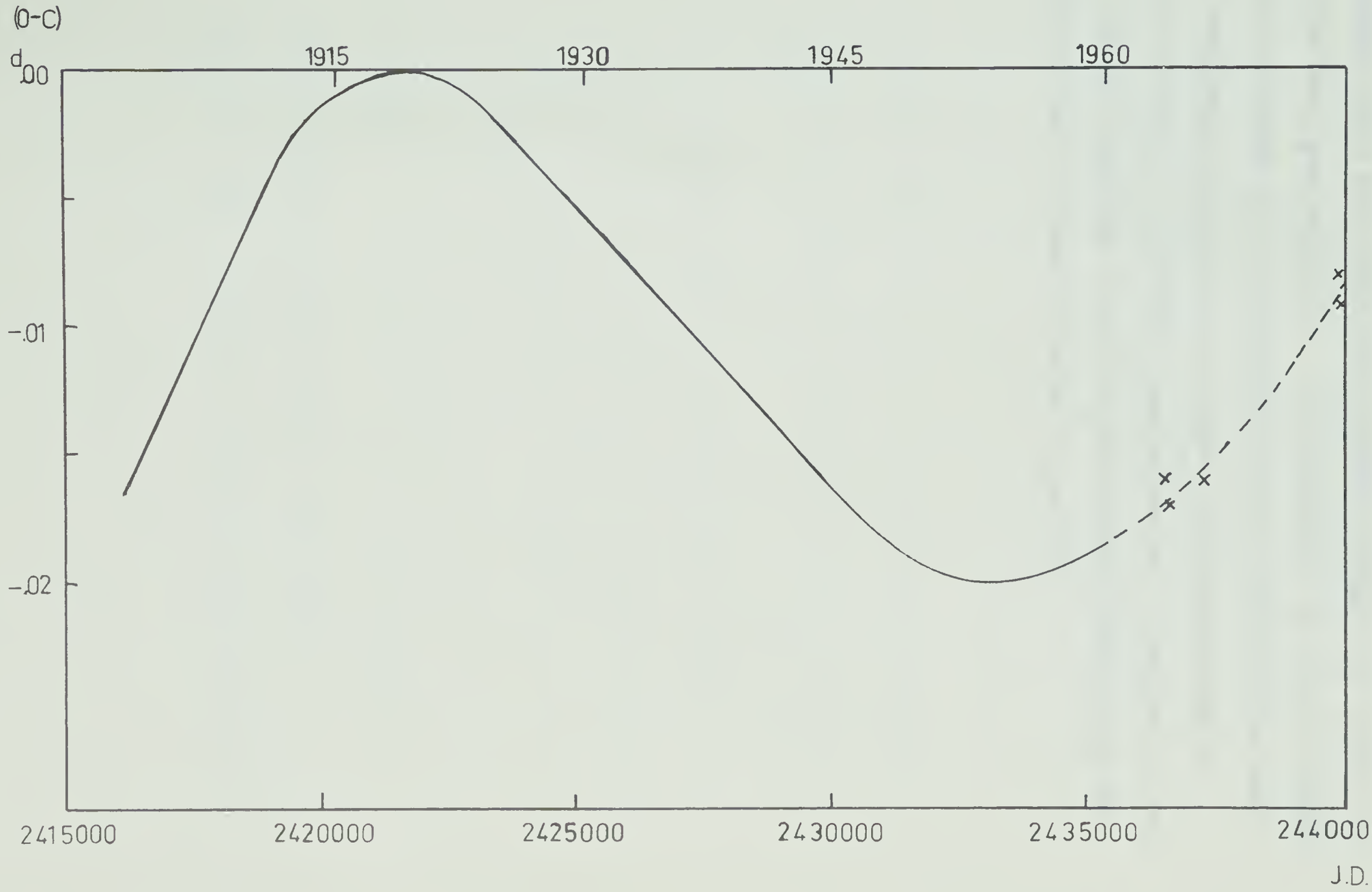

agreement with the theory that period changes are caused by a third body perturbation. An examination of the O-C graph, as it is formed up to the present time, indicates the need for continued observations of times of minimum light in order to come to a definite conclusion as to whether or not the period variation is cyclic, as well as determining the nature of any intrinsic changes in period.

LIST OF REFERENCES

(1) Weaver, H.F., Popular Astronomy, 54 212 (1946)

(2) Sidgwick, J.B., Amateur Astronomers Handbook, (Faber and Faber Ltd., London, 1961) 377

(3) de Vaucouleurs, G., Astronomical Photography, (Faber and Faber Ltd., London, 1961) I

(4) Stebbins, J. and Brown, F.C., Ap. J. 26 326 (1907)

(5) Wood, F.B., Ap. J. 112 196 (1950)

(6) Sky and Telescope, 34 367 (Dec. 1967)

(7) Johnson, H.L., Chapter 7, Astronomical Techniques, Ed. W.A. Hiltner, (Univ. of Chicago Press, 1962)

(8) Code, A.D., Chapter 2, Photoelectric Astronomy for Amateurs, Ed. F.B. Wood, (Macmillan Comp., New York, 1963)

(9) Hardie, R.H., Chapter 8, Astronomical Techniques, Ed. W.A. Hiltner, (Univ. of Chicago Press, 1962)

(10) Johnson, H.L., and Morgan, W.W., Ap. J. 117 313 (1953)

(11) Dugan, R.S., Ast. Nachr. 254 400 (1934)

(12) Swope, H., Princeton Contr. 13 (1933)

(13) Kordylewski, A.A.(c) 2 49

(14) Walter, K., Ast. Nachr. 253 9 (1934)

(15) Schmidt, H. and Schrick, K.W., Z. Astrophysik 41 I (1956)

(16) Binnendijk L., Properties of Double Stars, (Univ. of Pennsylvania Press, 1960) 243

(17) Bateson, F.M., Chapter 4, Photoelectric Astronomy for Amateurs, Ed. F.B. Wood, (Macmillan Comp., New York 1963)

(18) Binnendijk, L., Properties of Double Stars, (Univ. of Pennsylvania Press, 1960) 258

(19) Kopal, Z., Close Binary Systems, (John Wiley and Sons Inc., New York, 1959) 292

(20) Kuiper, G.P., Ap. J. 93 133 (1941)

(21) Kopal, Z., Close Binary Systems, (John Wiley and Sons Inc., New York, 1959) 467

(22) Eggen, O.J., Ap. J. 108 15 (1948)

(23) Schildt, J., Ap. J. 64 215 (1926)

(24) Schmidt, H. and Schrick, K.W., Z. Astrophysik 37 73 (1955)

(25) Payne Gaposchkin C., Meeting of American Astron. Soc. (1940)

(26) Binnendijk, L., A.J. 60 355 (1954)

(27) Muller, G. and Kempf, P., Ap. J. 17 201 (1903)

(28) Huffer, C.M., Ap. J. 79 369 (1934)

(29) Chou, K.C., A.J. 64 468 (1959)

(30) Kukarkin, B.V. and Parenago, P.P., General Catalogue of Variable Stars, (U.S.S.R. Academy of Sciences, 1948)

(31) Kopal, Z. and Shapely, M.B., Catalogue of the Elements of Eclipsing Binary Systems, Jodrell Bank Annals I 141 (1956)

(32) Payne Gaposchkin, C. and Gaposchkin, S., Variable Stars, Harvard Observatory Monographs 67

(33) Rakosch, K., Z. Astrophysik 50 178 (1960)

(34) Huffer, C.M., Ap. J. 103 I (1946)

(35) Schmidt, H. and Schrick, K.W., Z. Astrophysik 43 165 (1957)

(36) Wehlau, W. and Leung, K., J.R.A.S. Canada 56 105 (1962)

(37) Bookmeyer, B.B. A.J. 66 24 (1961)

(38) Blitzstein, W and Chou, K.C., A.J. 69 365 (1964)